

**TITLE:** Diagnostic test accuracy (DTA) of artificial intelligence in digital pathology: a systematic review, meta-analysis and quality assessment

**AUTHORS:** Clare McGenity<sup>1,2</sup>, Emily Clarke<sup>1,2</sup>, Charlotte Jennings<sup>1,2</sup>, Gillian Matthews<sup>2</sup>, Caroline Cartlidge<sup>1</sup>, Henschel Freduah-Agyemang<sup>1</sup>, Deborah Stocken<sup>1</sup>, Darren Treanor<sup>1,2,3,4</sup>

**AFFILIATIONS:**

<sup>1</sup> University of Leeds, Leeds, UK

<sup>2</sup> Leeds Teaching Hospitals NHS Trust, Leeds, UK

<sup>3</sup> Department of Clinical Pathology and Department of Clinical and Experimental Medicine, Linköping University, Linköping, Sweden

<sup>4</sup> Centre for Medical Image Science and Visualization (CMIV), Linköping University, Linköping, Sweden

**CORRESPONDING AUTHOR:**

Dr Clare McGenity

Email: c.m.mcgenity@leeds.ac.uk

**ABSTRACT:**

**Background / Objectives**

Ensuring the diagnostic performance of AI models before their introduction into clinical practice is key to the safe and successful adoption of these technologies. Studies reporting AI applied to digital pathology images for a variety of diagnostic purposes have rapidly increased in number in recent years. The aim of this work is to provide an overview of the diagnostic accuracy of AI in digital pathology images from all areas of pathology.

**Methods**

This systematic review and meta-analysis included diagnostic accuracy studies using any type of artificial intelligence applied to whole slide images (WSIs) in any disease type. The reference standard was diagnosis through histopathological assessment and / or immunohistochemistry. Searches were conducted in PubMed, EMBASE and CENTRAL in June 2022. We identified 2976 studies, of which 100 were included in the review and 48 in the full meta-analysis. Risk of bias and concerns of applicability were assessed using the QUADAS-2 tool. Data extraction was conducted by two investigators and meta-analysis was performed using a bivariate random effects model.

**Results**

100 studies from a range of countries were identified for inclusion, equating to over 152,000 whole slide images (WSIs) and representing a variety of disease types. Of these, 48 studies were included in the meta-analysis. These studies reported a mean sensitivity of 96.3% (CI 94.1-97.7) and mean specificity of 93.3% (CI 90.5-95.4) for AI. There was substantial heterogeneity in study design and all 100 studies identified for inclusion had at least one area at high or unclear risk of bias.

**Conclusions**

This review provides a broad overview of AI performance across applications in whole slide imaging. However, there is huge variability in study design and available performance data, with details around the conduct of the study and make up of the datasets frequently missing. Overall, AI offers good accuracy when applied to WSIs but requires more rigorous evaluation of its performance.

## INTRODUCTION:

The last decade of artificial intelligence (AI) research has seen exciting advancements in the automation of diagnostic tasks to assist the pathologist in their assessment whole slide images (WSIs).<sup>1-4</sup> AI has been applied digital pathology for many disease types to perform diagnostic tasks with some impressive successes.<sup>5-8</sup> In 2017, Bejnordi et al. described 32 AI models developed for breast cancer detection in lymph nodes through the CAMELYON16 grand challenge. The best model achieved an area under the curve (AUC) of 0.994 (95% CI 0.983-0.999).<sup>9</sup> A study by Lu et al. in 2021 described AI applied to determining tumour origin in cases of cancer of unknown primary (CUP).<sup>10</sup> Their model achieved an AUC of 0.8 and 0.93 for top-1 and top-3 tumour accuracies respectively on an external test set. AI has also been applied to making predictions, such as determining the 5-year survival in colorectal cancer patients and the mutation status across multiple tumour types.<sup>11,12</sup>

Several recent reviews have examined the performance of AI in subspecialties of pathology. In 2020, Thakur et al. identified 30 studies of colorectal cancer for review with some demonstrating strong performance, although the overall scale of studies was small and limited in their clinical application.<sup>13</sup> Similarly in breast cancer, Krithiga et al. examined studies image analysis techniques were used to detect, segment and classify disease, with reported accuracies ranging from 77 to 98%.<sup>14</sup> Other recent reviews have examined applications in liver pathology, skin pathology and kidney pathology with evidence of promising performance from some AI models.<sup>15-17</sup> Additionally, Rodriguez et al. performed a broader review of AI applied to WSIs and identified 26 studies for inclusion with a focus on slide level diagnosis.<sup>18</sup> They found substantial heterogeneity in the way performance metrics were presented and limitations in the ground truth used within studies.

Despite these developments, examples of routine clinical use of these technologies remain rare in histopathology and there are concerns around the performance, evidence quality and risk of bias for medical AI studies in general.<sup>19-21</sup> However, in the face of an increasing pathology workforce crisis, the prospect of tools that can assist and automate tasks is appealing.<sup>22,23</sup> Challenging workflows and long waiting lists mean that substantial patient benefit could be realised if AI was successfully harnessed to assist in the workflow.

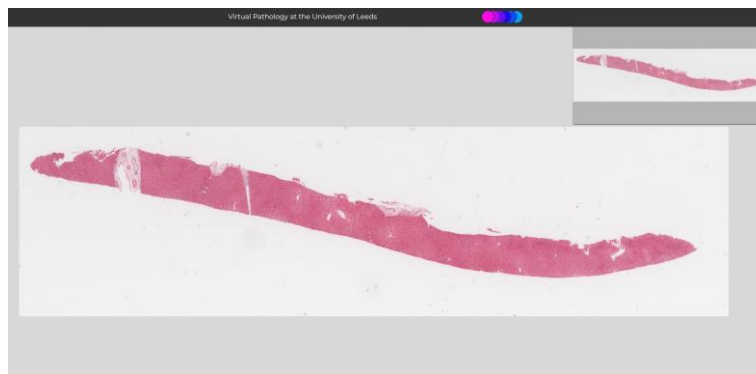


**Figure 1** – Example whole slide image (WSI) of a liver biopsy specimen at low magnification. These are high resolution digital pathology images viewed by a pathologist on a computer to make a diagnostic assessment. Image courtesy of [www.virtualpathology.leeds.ac.uk](http://www.virtualpathology.leeds.ac.uk)<sup>24</sup>

This review provides an overview of performance of these diagnostic tools across histopathology. The objective of this review was to determine the diagnostic test accuracy of artificial intelligence solutions applied to whole slide images to diagnose disease.

## METHODS:

This systematic review and meta-analysis was conducted in accordance with the guidelines for the “Preferred Reporting Items for Systematic Reviews and Meta-Analyses” extension for diagnostic accuracy studies (PRISMA-DTA).<sup>25</sup> The protocol for this review is available

### Eligibility Criteria

Studies reporting the diagnostic accuracy of AI models applied to WSIs for any disease diagnosed through histopathological (surgical pathology) assessment and / or immunohistochemistry were sought. The primary outcome was the diagnostic accuracy of AI tools in detecting disease or classifying subtypes of disease. The index test was any AI model applied to whole slide images. The reference standard was any diagnostic histopathological interpretation by a pathologist and / or immunohistochemistry.

Studies were excluded where the outcome was a prediction of patient outcomes, treatment response, molecular status, whilst having no detection or classification of disease. Studies of cytology, autopsy and forensics cases were excluded. Studies grading, staging or scoring disease, but without results for detection of disease or classification of disease subtypes were also excluded. Studies examining modalities other than whole slide imaging or studies where WSIs were mixed with other imaging formats were also excluded.

### Data sources and search strategy

Electronic searches of PubMed, EMBASE and CENTRAL were performed from inception to 20<sup>th</sup> June 2022. Searches were restricted to English language and human studies. There were no restrictions on the date of publication. The full search strategy is available in the supplementary materials. Citation checking was also conducted.

### Study selection

Two investigators (C.M. and H.F.A.) independently screened titles and abstracts against a predefined algorithm to select studies for full text review. The screening tool is available in the supplementary materials. Disagreement regarding study inclusion was resolved by discussion with a third investigator (D.T.). Full text articles were reviewed by two investigators (C.M. and E.L.C.) to determine studies for final inclusion.

### Data extraction and quality assessment

Data collection for each study was performed independently by two reviewers using a predefined electronic data extraction spreadsheet. Every study was reviewed by the first investigator (C.M.) and a team of four investigators were used for second independent review (E.L.C. / C.J. / G.M. / C.C.). Data extraction obtained the study demographics; disease examined; pathological subspecialty; type of AI; type of reference standard; datasets details; split into train / validate / test sets and test statistics to construct 2x2 tables of the number of true-positives (TP), false positives (FP), false negatives (FN) and true negatives (TN). An indication of best performance with any diagnostic accuracy metric provided was recorded for all studies. Corresponding authors of the primary research were contacted to obtain missing performance data.

At the time of writing, the QUADAS-AI tool was still in development and so could not be utilised.<sup>26</sup> Therefore, a tailored QUADAS-2 tool was used to assess the risk of bias and any applicability concerns for the included studies.<sup>27,28</sup> Further details of the quality assessment process can be found in the supplementary materials.

### Statistical analysis

Data analysis was performed using MetaDTA: Diagnostic Test Accuracy Meta-Analysis v2.01 Shiny App to generate forest plots, summary receiver operating characteristic (SROC) plots and summary sensitivities and specificities, using a bivariate random effects model.<sup>29,30</sup> If available, 2x2 tables were used to include studies in the meta-analysis to provide an indication of diagnostic accuracy demonstrated in the study. Where unavailable, this data was requested from authors or calculated from other metrics provided. Where only multiclass data was available, this was combined into a 2x2 format, unless negative results categories were unavailable (e.g. for multiple comparisons between disease types only).

## RESULTS

### Study selection

Searches identified 2976 abstracts, of which 1666 were screened after duplicates were removed. 296 full text papers were reviewed for potential inclusion. 100 studies met the full inclusion criteria for inclusion in the review, with 48 studies included in the full meta-analysis (**Figure 1**).

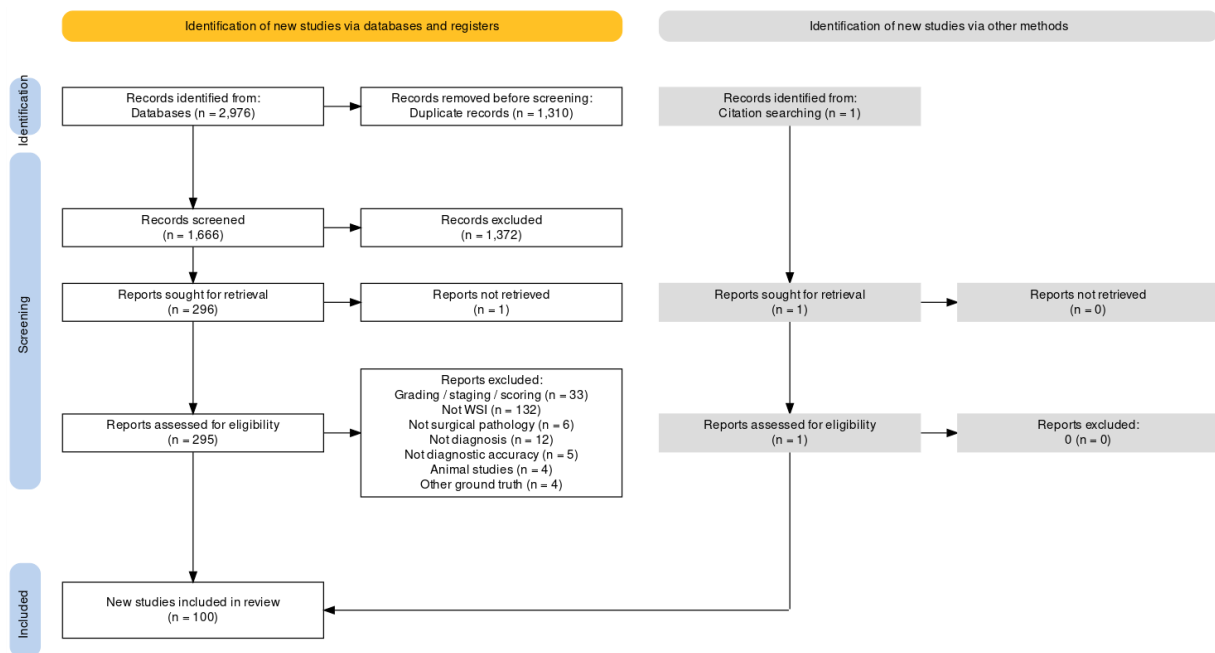


**Figure 2** – Study selection flow diagram. Generated using PRISMA2020 at [https://estech.shinyapps.io/prisma\\_flowdiagram/](https://estech.shinyapps.io/prisma_flowdiagram/)<sup>31</sup>

### Study characteristics

Study characteristics are presented in **Tables 1-8**. Further details, including funding sources for the studies can be found in the supplementary materials. Study characteristics are presented by pathological subspecialty for all 100 studies identified for inclusion. **Table 1** and **Table 2** show characteristics for breast pathology and cardiothoracic pathology studies respectively. **Table 3** and **Table 4** are characteristics for dermatopathology and hepatobiliary pathology studies respectively. **Table 5** and **Table 6** have characteristics for gastrointestinal and urological pathology studies respectively. Finally, **Table 7** outlines characteristics for studies with multiple pathologies examined and for other pathologies such as gynaepathology, haematopathology, head and neck pathology, neuropathology, paediatric pathology, bone pathology and soft tissue pathology. Studies from Europe, Asia, Africa, North America, South America and Australia / Oceania were all represented within the review, with the largest numbers of studies coming from the USA and China.

Table 1. Characteristics of breast pathology studies										
First author, year & reference	Location	Index test	Disease studied	Reference standard	Data sources	Training set details	Validation set details	Test set details	External validation	Unit of analysis
Cengzig (2022) <sup>32</sup>	Turkey	CNN	Breast cancer	Not stated	Not stated	296,675 patches		101,706 patches	Unclear	Patch / Tile
Choudhary (2021) <sup>33</sup>	India, USA	CNN (VGG19, ResNet54, ResNet50)	Breast cancer	Pathologist annotations, slide diagnoses	IDC dataset	194,266 patches		83,258 patches	No	Patch / Tile
Cruz-Roa (2018) <sup>34</sup>	Colombia, USA	FCN (HASHI)	Breast cancer	Pathologist annotations	Hospital of the University of Pennsylvania; University Hospitals Case Medical Centre / Case Western Reserve University; Cancer Institute of New Jersey; TCGA	698 cases	52 cases	195 cases	Yes	Pixel
Cruz-Roa (2017) <sup>35</sup>	Colombia, USA	CNN (ConvNet)	Breast cancer	Pathologist annotations	University of Pennsylvania Hospital; University Hospitals Case Medical Centre / Case Western Reserve University; Cancer Institute of New Jersey; TCGA	349 patients	40 patients	216 patients	Yes	Pixel
Hameed (2020) <sup>36</sup>	Spain / Columbia	Ensemble of fine-tuned VGG16 and fine-tuned VGG19 CNN models	Breast cancer	Pathologist labels / annotations	Colsanitas Colombia University	540 images/patches	135 images/patches	170 images/patches	No	Patch / Tile
Jin (2020) <sup>37</sup>	Canada	U-net CNN (ConcatNet)	Breast cancer	Labels	PatchChamelyon dataset, Open-source dataset from PMID 27563488, Warwick dataset	262,144 patches + 538 images	32,768 patches	32,768 patches	No	Patch / Tile
Johny (2021) <sup>38</sup>	India	Custom deep CNN	Breast cancer	Pathologist patch labels	PatchCamelyon Dataset	262,144 patches		65,536 patches	No	Patch / Tile
Kanavati (2021) <sup>39</sup>	Japan	CNN tile classifier (EfficientNetB1) + RNN tile aggregator	Breast cancer	Diagnostic review by pathologists	International University of Health and Welfare, Mita Hospital; Sapporo-Kosei General Hospital.	1652 WSIs	90 WSIs	1930 WSIs	Yes	Slide
Khalil (2022) <sup>40</sup>	Taiwan	Modified FCN	Breast cancer	Pathologist annotations, IHC.	National Taiwan University Hospital dataset	68 WSIs		26 WSIs	No	Slide
Lin (2019) <sup>41</sup>	Hong Kong / China / UK	Modified FCN	Breast cancer	Slide level labels, pathologist annotations	Camelyon dataset	202 WSIs	68 WSIs	130 WSIs	No	Slide
Roy (2021) <sup>42</sup>	India / Germany	Multiple machine learning classifiers (CatBoost, others)	Breast cancer	Unclear	IDC Breast Histopathology Image Dataset		Unclear		No	Patch / Tile
Sadeghi (2019) <sup>43</sup>	Germany / Austria	CNN	Breast cancer	Pathologist supervised annotations, IHC	Camelyon 17 dataset, Camelyon 16 dataset	400 WSIs	100 WSIs	20,000 patches	No	Patch / Tile
Steiner (2018) <sup>44</sup>	USA	CNN (LYNA - Inception framework)	Breast cancer	Pathologist review, IHC	Camelyon; Expired clinical archive blocks from 2 sources	215 WSIs	54 WSIs	70 WSIs	Yes	Slide
Valkonen (2017) <sup>45</sup>	Finland	Random forest	Breast cancer	Pathologist WSI annotations	Camelyon16 dataset	1,000,000 patches		270 WSIs leave-one-out cross validation	Yes	Patch / Tile
Wang Q (2021) <sup>46</sup>	China	SoMIL) + adaptive aggregator + RNN	Breast cancer	WSI labels, pixel level annotations of metastases	Camelyon-16; MSK breast cancer metastases dataset.	289 WSIs		240 WSIs	Yes	Slide
Wu (2020) <sup>47</sup>	USA	ROI classifier + Tissue segmentation CNN + Diagnosis classifier SVM	Breast cancer	Pathologist pixel labels	R01 CA140560 breast cancer biopsy dataset	58 ROIs		Cross validation 428 ROIs	Unclear	Other (ROIs)

Table 2. Characteristics of cardiothoracic pathology studies										
First author, year & reference	Location	Index test	Disease studied	Reference standard	Data sources	Training set details	Validation set details	Test set details	External validation	Unit of analysis
Chen (2021) <sup>48</sup>	Taiwan	CNN	Lung cancer	Pathologist diagnosis. Slide level labels.	Taipei Medical University Hospital; Taipei Muncipal Wanfang Hospital; Taipei Medical University Shuang-Ho Hospital; TCGA.	5045 WSIs	561 WSIs	2441 WSIs	Yes	Slide
Chen (2022) <sup>49</sup>	China	CNN (EfficientNetB5)	Lung cancer	Pathologist annotations	Hospital of Sun Yat-sen University; Shenzhen People's Hospital; Cancer Centre of Guangzhou Medical University	813 cases train & validate		1101 cases	Yes	Slide
Coudray (2018) <sup>50</sup>	USA, Greece	CNN (Inception v3)	Lung cancer	Pathologist labels	TCGA, New York University	1157 WSIs	234 WSIs	584 WSIs	Yes	Slide
Dehkharghanian (2021) <sup>51</sup>	Canada, USA	DNN (KimiaNet)	Lung cancer	WSI diagnostic label	TCGA; Grand River Hospital, Kitchener, Canada.	575 WSIs	79 WSIs	81 WSIs	Yes	Patch / Tile
Kanavati (2020) <sup>52</sup>	Japan	CNN (EfficientNet-B3)	Lung cancer	Pathologist review and annotations	Kyushu Medical Centre; Mita Hospital; TCGA; TCIA	3554 WSIs	150 WSIs	2170 WSIs	Yes	Slide
Wang X (2020) <sup>53</sup>	China / Hong Kong / UK	FCN + Random Forest classifier	Lung cancer	Pathologist annotations, WSI labels.	Sun Yat-sen University Cancer Centre (SUCC); TCGA	1154 WSIs		285 WSIs	Yes	Slide
Wei (2019) <sup>54</sup>	USA	CNN (ResNet)	Lung cancer	Pathologist WSI labels	Dartmouth-Hitchcock Medical Centre (DHMC)	245 WSIs	34 WSIs	143 WSIs	No	Slide
Yang (2021) <sup>55</sup>	China	CNN (EfficientNetB5; ResNet50)	Lung cancer	Pathologist diagnosis, IHC, medical records.	Sun Yat-sen University; Shenzhen People's Hospital; TCGA.	511 WSIs	115 WSIs	1067 WSIs	Yes	Patch / Tile
Zhao (2021) <sup>56</sup>	China	Combined (MR-EM-CNN + HMS + RNN + RMDL)	Lung cancer	Pathologist annotations, patch labels.	TCGA	1481 WSIs	321 WSIs	323 WSIs	No	Slide
Zheng (2022) <sup>57</sup>	USA	CNN (GTP: Graph transformer + node representation connectivity information + feature generation and contrastive learning)	Lung cancer	Pathologist annotations. WSI level labels.	Clinical Proteomic Tumor Analysis Consortium (CPTAC), TCGA & the National Lung Screening Trial (NLST)	2071 WSIs 5 fold cross validation		2082 WSIs	Yes	Slide
Uegami (2022) <sup>58</sup>	Japan	CNN (ResNet18) + K means clustering + pathologist clustering + transfer learning	Interstitial lung disease	Pathologist diagnosis	1 institute (unclear)	126 cases (additional cases for pretraining)	54 cases	180 WSIs, 51 cases	No	Patch / Tile

Table 3. Characteristics of dermatopathology studies										
First author, year & reference	Location	Index test	Disease studied	Reference standard	Data sources	Training set details	Validation set details	Test set details	External validation	Unit of analysis
Kimeswenger (2020) <sup>59</sup>	Austria / Switzerland	CNN + ANN (Feature constructor ImageNet CNN + classification ANN (based on multiple instance learning with attention classifier))	Basal cell carcinoma	Categorised by pathologist	Kepler University Hospital; Medical University of Vienna.	688 WSIs		132 WSIs	No	Patch / Tile
Alheejawi (2021) <sup>60</sup>	Canada, India	CNN	Melanoma	MART-1 stained images	Cross Cancer Institute, University of Alberta, Edmonton, Canada	70 960x960 pixel images	15 960x960 pixel images	15 960x960 pixel images	No	Pixel
De Logu (2020) <sup>61</sup>	Italy	CNN (Inception ResNet v2)	Melanoma	Pathologist review	University of Florence, University Hospital of Siena, Institute of Biomolecular Chemistry, National research Council	45 WSIs	15 WSIs	40 WSIs	No	Patch / Tile
Hekler (2019) <sup>62</sup>	Germany	CNN (ResNet50)	Melanoma	Image labels	Dr Dieter Krahl institute, Heidelberg	595 cropped images		100 cropped images	No	Patch / Tile
Hohn (2021) <sup>63</sup>	Germany	CNN (ResNeXt50)	Melanoma	Pathologist diagnosis	Two laboratories unspecified	232 WSIs	67 WSIs	132 WSIs	No	Slide
Li (2021) <sup>64</sup>	China	CNN (ResNet50)	Melanoma	Pathologist WSI annotations	Central South University Xiangya Hospital; TCGA	491 WSIs	105 WSIs	105 WSIs	No	Slide
Wang L (2020) <sup>65</sup>	China	CNN for patch-level classification (VGG16) & random forest for WSI-level classification	Melanoma	Pathologist diagnosis, consensus, IHC, annotations.	Zhejiang University School of Medicine, Ninth People's Hospital of Shanghai	105415 patches	1962 patches	118,123 patches	Yes	Patch / Tile
del Amor (2021) <sup>66</sup>	Spain	CNN (VGG16, ResNet50, InceptionV3, MobileNetV2)	Spitzoid skin tumours	Pathologist annotations	CLARIFYv1	36 WSIs 5 fold cross validation of training set		15 WSIs	No	Unclear

Table 4. Characteristics of hepatobiliary pathology studies										
First author, year & reference	Location	Index test	Disease studied	Reference standard	Data sources	Training set details	Validation set details	Test set details	External validation	Unit of analysis
Aatresh (2021) <sup>67</sup>	India	CNN (LiverNet)	Liver cancer	Pathologist annotations	Kasturba Medical College (KMC); TCGA	5 fold cross-validation	5450 samples		No	Patch / Tile
Chen (2020) <sup>68</sup>	China	CNN (Inception V3)	Liver cancer	Labels	TCGA, Sir Run-Run Shaw Hospital	278 WSIs	56 WSIs	258 WSIs	Yes	Patch / Tile
Kiani (2020) <sup>69</sup>	USA	CNN (Densenet)	Liver cancer	Pathologist diagnosis, consensus, IHC, special stains	TCGA; Stanford whole-slide image dataset	20 WSIs	50 WSIs	106 WSIs	Yes	Slide
Yang (2022) <sup>70</sup>	Taiwan	Feature Aligned Multi-Scale Convolutional Network (FA-MSCN)	Liver cancer	Pathologist labels and ROIs	Unclear	20 WSIs		26 WSIs	Unclear	Unclear
Schau (2020) <sup>71</sup>	USA / Thailand	CNNs (Inception v4)	Liver metastases	Pathologist labels, annotations	OHSU Knight BioLibrary	200 WSIs		85 WSIs	No	Patch / Tile
Fu (2021) <sup>72</sup>	China	Inception v3 CNN (patch-level classification), lightGBM model (WSI-level classification), and U-Net CNN (patch-level segmentation)	Pancreatic cancer	Pathologist annotations, labels	Peking Union Medical College Hospital (PUMCH); TCGA	79,588 patches	9952 patches	9,948 patches + 52 WSIs	Yes	Slide
Naito (2021) <sup>73</sup>	Japan	CNN (EfficientNetB1)	Pancreatic cancer	Pathologist review, pathologist annotations	Kurume University	372 WSIs	40 WSIs	120 WSIs	No	Slide
Song (2013) <sup>74</sup>	South Korea	Bayesian classifier; k-NN; SVM; ANN.	Pancreatic neoplasms	Unclear	Pathology department of Yeognam University	240 patches		160 patches	No	Patch / Tile

Table 5. Characteristics of gastrointestinal pathology studies										
First author, year & reference	Location	Index test	Disease studied	Reference standard	Data sources	Training set details	Validation set details	Test set details	External validation	Unit of analysis
Sali (2020) <sup>75</sup>	USA	CNN and Random forest / SVM / k-means / GMM	Barrett's Oesophagus	Pathologist consensus; pixel-wise annotations	Hunter Holmes McGuire Veterans Affairs Medical Center	115 WSIs	535 WSIs	10 fold cross validation	No	Slide
Syed (2021) <sup>76</sup>	USA / Pakistan / Zambia / UK	4 CNN models: ResNet50, ResNet50 multi-zoom, shallow CNN, an ensemble of ResNet50 and shallow CNN.	Coeliac & Environmental Enteropathathy	Slide level diagnosis, IHC, Patch labels.	Aga Khan University; University of Zambia & University Teaching Hospital Zambia; University of Virginia, USA.	231 WSIs	115 WSIs	115 WSIs	Unclear	Slide
Nasir-Moin (2021) <sup>77</sup>	USA	CNN (ResNet18)	Colorectal adenoma / polyps	Pathologist consensus	Dartmouth-Hitchcock Medical Centre (DHMC), Prior validation on 24 US institutions	508 WSIs		100 WSIs + Previous validation 238 WSIs	Yes	Slide
Song (2020a) <sup>78</sup>	China	CNN (DeepLab v2 with ResNet34)	Colorectal adenoma / polyps	Pathologist labels	Chinese People's Liberation Army General Hospital (PLAGH); China-Japan Friendship Hospital (CJFH); Cancer Hospital, Chinese Academy of Medical Science (CH).	177 WSIs	40 WSIs	362 WSIs	Yes	Slide
Wei (2020) <sup>79</sup>	USA	CNN (ResNet)	Colorectal adenoma / polyps	Pathologist annotations	Dartmouth-Hitchcock Medical Centre (DHMC); External set 24 institutions	326 WSIs	25 WSIs	395 WSIs	Yes	Slide
Feng (2021) <sup>80</sup>	China, USA, South Korea	Ensemble of 8 networks: modified U-Net CNNs with VGG-16 or VGG-19 backbones	Colorectal cancer	Pixel annotations, pathologist labels	DigestPath 2019 Challenge (task 2)	750 WSIs		250 WSIs	No	Unclear
Haryanto (2021) <sup>81</sup>	Indonesia	Conditional Sliding Window (CSW) algorithm used to generate images for CNN 7-5-7	Colorectal cancer	Pathologist labels & annotations	Warwick dataset; University of Indonesia		Unclear		Unclear	Unclear
Sabol (2020) <sup>82</sup>	Slovakia / Japan	CNN + X-CFCMC	Colorectal cancer	Annotations	Publicly available dataset from Kather et al.		10 fold cross validation	5000 tiles	No	Patch / Tile
Schrammen (2022) <sup>83</sup>	Germany / Netherlands / UK	Single neural network (SLAM - based on ShuffleNet)	Colorectal cancer	Patient/slide level labels	DACHS study, YCR-BCIP	2448 cases		889 cases	Yes	Slide
Tsuneki (2021) <sup>84</sup>	Japan	CNN (EfficientNetB1)	Colorectal cancer	Pathologist diagnosis & annotations	Wajiro, Shinmizumaki, Shinkomonji, and Shinyukuhashi hospitals, Fukuoka; Mita Hospital, Tokyo	680 WSIs	68 WSIs	1799 WSIs	Yes	Slide
Wang KS (2017) <sup>85</sup>	China / USA	CNN (Inception V3)	Colorectal cancer	Pathologist consensus & labels	14 hospitals / sources	559 WSIs	283 WSIs	At least 13,838 WSIs	Yes	Patch / Tile
Wang C (2017) <sup>86</sup>	China	CNN (bilinear)	Colorectal cancer	Annotations	University Medical Center Mannheim, Heidelberg	See test	See test	5 fold cross validation on 1000 patches	No	Patch / Tile
Xu (2021) <sup>87</sup>	China	Dual resolution deep learning network with self-attention mechanism (DRSNet)	Colorectal cancer	Pathologist annotations; Patch labels; Pathologist pixel annotations.	TCGA; Affiliated Cancer Hospital and Institute of Guangzhou Medical University (ACHIGMU)	100,000 patches	40,000 patches	40,000 patches + 40,000 patches (ext)	Yes	Patch / Tile
Zhou (2021) <sup>88</sup>	China / Singapore	CNN (ResNet) + Random Forest	Colorectal cancer	Pathologist slide labels, reports, annotations & consensus	TGCA, Hospital of Zhejiang University, Hospital of Soochow University, Nanjing First Hospital	950 WSIs		TCGA 396 WSIs; Hospitals set: 50 WSIs	Yes	Slide
Ashraf (2022) <sup>89</sup>	South Korea	CNN (DenseNet-201)	Gastric cancer	Pathologist review & annotations	Seegene Medical Foundation in South Korea and Camyelon	723 WSIs (primary model), 262,11 patches (lymph node model)	91 WSIs (primary model), 32,768 patches (LN model)	91 WSIs (primary model), 32,768 patches (LN model)	No	Patch
Cho (2019) <sup>90</sup>	South Korea	CNN (AlexNet; ResNet50; Inception-v3)	Gastric cancer	Labels	TCGA-STAD; SSMH Seoul St. Mary's Hospital dataset		10 fold cross validation		Yes	Slide
Ma (2020) <sup>91</sup>	China	CNN (modified InceptionV3) + random forest classifier	Gastric cancer	Pathologist annotations	Ruijin Hospital	534 WSIs	76 WSIs	153 WSIs	No	Slide
Rasmussen (2020) <sup>92</sup>	Canada	CNN (DenseNet169)	Gastric cancer	Pathologist annotations	Queen Elizabeth II Health Sciences Centre and Dalhousie University; Sunnybrook Health Science Centre, University of Toronto	14,266 patches	1585 patches	971 patches + external 814 patches	Yes	Patch / Tile
Song (2020b) <sup>93</sup>	China / USA	CNN (Multiple models) and random forest	Gastric cancer	Pathologist pixel level annotations	PLAGH dataset; Multicentre dataset (PUMCH, CHCAMS & Pekin Union Medical College)	2860 WSIs	300 WSIs	4993 WSIs	Yes	Slide
Tung (2022) <sup>94</sup>	Taiwan	CNN (YOLOv4)	Gastric cancer	Pathologist annotations	Taiwan Cancer Registry Database	2200 image tiles		550 image tiles	No	Patch / Tile

Wang S (2019) <sup>95</sup>	China	Recalibrated multi-instance deep learning method (RMDL)	Gastric cancer	Pathologist pixel annotations	Sun Yat-sen University	408 WSIs		200 WSIs	No	Slide
Ba (2021) <sup>96</sup>	China	CNN (ResNet50)	Gastritis	Pathologist review & pixel annotations	Chinese People's Liberation Army General Hospital	1008 WSIs	100 WSIs	142 WSIs	No	Slide
Steinbuss (2020) <sup>97</sup>	Germany	CNN (Xception)	Gastritis	Diagnoses – modified Sydney Classification, pathologist annotations	Institute of Pathology, University Clinic Heidelberg	825 patches	196 patches	209 patches	No	Patch / Tile
Iizuka (2020) <sup>98</sup>	Japan	Inception V3 CNN with max-pooling or RNN aggregator	Multiple (Colorectal cancer & Gastric tumours)	Pathologist annotations	Hiroshima University Hospital dataset; Haradai Hospital dataset; TCGA dataset	3,628 WSIs stomach, 3,536 WSIs colon		1,475 stomach, 1,574 colon (from 3 test sets)	Yes	Slide

**Table 6. Characteristics of urological pathology studies**

First author, year & reference	Location	Index test	Disease studied	Reference standard	Data sources	Training set details	Validation set details	Test set details	External validation	Unit of analysis
da Silva (2021) <sup>99</sup>	Brazil, USA	CNN (Paige Prostate 1.0)	Prostate cancer	Pathologist consensus, IHC	Instituto Mario Penna, Brazil	Prior study: trained on 2000 WSIs		661 WSIs (579 part specimens)	Yes	Other (part specimen level)
Duran-Lopez (2021) <sup>100</sup>	Spain	CNN (PROMETEO) + Wide and deep neural network	Prostate cancer	Pathologist pixel annotations	Pathological Anatomy Unit of Virgen de Valme Hospital, Spain	5 fold cross validation		332 WSIs	No	Slide
Esteban (2019) <sup>101</sup>	Spain	Optical density granulometry-based descriptor + Gaussian processes	Prostate cancer	Pathologist pixel annotations	SICAPv1 database; Prostate cancer database by Gertych et al.	60 WSIs 5 fold cross validation		19 WSIs + 593 patches	Yes	Patch / Tile
Han (2020a) <sup>102</sup>	Canada	7 ML approaches. Best: Transfer learning with TCMs	Prostate cancer	Pathologist annotations / supervision	Western University	286 WSIs cross validation for train / test (leave one out)		13 WSIs	No	Patch / Tile
Han (2020b) <sup>103</sup>	Canada	Traditional ML and 14 texture features extracted from TCMs; Transfer learning with pretrained AlexNet fine-tuned by TCM ROIs; Transfer learning with pretrained AlexNet fine-tuned with raw image ROIs	Prostate cancer	Pathologist annotations / supervision	Western University	286 WSIs cross validation for train / test (leave one out)		13 WSIs	No	Patch / Tile
Huang (2021) <sup>104</sup>	USA	CNN (U-Net gland segmenter) + CNN feature extractor & classifier	Prostate cancer	Pathologist review, patch annotations using ISUP criteria.	University of Wisconsin Health System	838 WSIs		162 WSIs	No	Other (patch-pixel level)
Swiderska-Chadaj (2020) <sup>105</sup>	Netherlands / Sweden	CNN (U-Net, DenseNetFCN, EfficientNet)	Prostate cancer	Slide level labels, pathologist annotations	The Penn State Health Department of Pathology; PAMM Laboratorium voor Pathologie; Radboud University Medical Center.	264 WSIs	60 WSIs + 96 WSIs post processing optimisation	297 WSIs	Yes	Slide
Tsuneki (2022) <sup>106</sup>	Japan	Transfer learning (TL-colon poorly ADC-2 (20x,512)); CNN (EfficientNetB1 20x, 512); CNN (EfficientNetB1 (10x,224)	Prostate cancer	Pathologist diagnosis & consensus	Wajiro, Shimizumaki, Shinkomonji, and Shinyukuhashi hospitals, Fukuoka; TGCA	1122 WSIs	60 WSIs	2512 WSIs	Yes	Slide
Abdeltawab (2021) <sup>107</sup>	USA, UAE	CNN (pyramidal)	Renal cancer	Pathologist review & annotations	Indiana University, USA	38 WSIs	6 WSIs	20 WSIs	No	Pixel
Fenstermaker (2020) <sup>108</sup>	USA	CNN	Renal cancer	Pathology report	TCGA	15,168 patches train / validate		4,286 patches	No	Patch / Tile
Tabibu (2019) <sup>109</sup>	India	CNNs (ResNet18 & 34) + SVM (DAG-SVM)	Renal cancer	Clinical information inc. pathology reports	TCGA (TCGA-KIRC; TGCA-KIRP; TCGA-KICH; normal images from TCGA)	1474 WSIs	317 WSIs	314 WSIs	Yes	Slide
Zhu (2021) <sup>110</sup>	USA	CNN (ResNet-18) + Decision Tree	Renal cancer	Pathologist annotations	1. Resections from DHMC, 2. The Cancer Genome Atlas (TCGA) (open), 3. Biopsies from DHMC	385 WSIs	23 WSIs	1074 WSIs	Yes	Slide

Table 7. Characteristics of other pathology / multiple pathology studies										
First author, year & reference	Location	Index test	Disease studied	Reference standard	Data sources	Training set details	Validation set details	Test set details	External validation	Unit of analysis
BenTaieb (2017) <sup>111</sup>	Canada	K means + LSMV	Ovarian cancer	Pathologist consensus	Not stated	68 WSIs		65 WSIs	No	Slide
Shin (2020) <sup>112</sup>	South Korea	CNN (Inception V3)	Ovarian cancer	Pathologist diagnosis	TCGA; Ajou University Medical Centre	7245 patches (114 patients)		3051 patches	Yes	Patch / Tile
Sun (2020) <sup>113</sup>	China	CNN (HIENet)	Endometrial cancer	Pathologist consensus, patch labels	2 dataset from Hospital of Zhengzhou University	10 fold cross validation on 3300 patches		200 patches	No	Patch / Tile
Yu (2020) <sup>114</sup>	USA	CNN (VGGNet, GoogLeNet; AlexNet)	Ovarian cancer	Pathology reports and pathologist review	TCGA	1100 WSIs		275 WSIs	No	Slide
Achi (2019) <sup>115</sup>	USA	CNN	Lymphoma	Labels	Virtual pathology at University of Leeds, Virtual Slide Box University of Iowa Kurume University	1856 40x40 patches	464 patches	240 patches	No	Patch / Tile
Miyoshi (2020) <sup>116</sup>	Japan / USA	deep neural network classifier with averaging method	Lymphoma	Pathologist annotations, IHC		Unclear	Unclear	100 patches (each at 5x, 20x and 40x)	No	Patch / Tile
Mohlman (2020) <sup>117</sup>	USA	deep densely connected CNN	Lymphoma	Unclear - likely slide diagnosis	University of Utah dataset, Mayo Clinic Rochester dataset	8796 patches		2037 patches	No	Patch / Tile
Sryrykh (2020) <sup>118</sup>	France	CNNs ("Several Deep CNNs" + Bayesian Neural Network)	Lymphoma	Slide diagnosis, IHC, patch labels	Toulouse University Cancer Institute, France; Dijon University Hospital, France.	221 WSIs	111 WSIs	159 WSIs	No	Slide
Yu (2019) <sup>119</sup>	USA	CNN (VGGNet & others)	Lymphoma	Pathologist consensus, IHC	TCGA & International Cancer Genoma Consortium (ICGC)	707 patients		302 patients	Yes	Patch / Tile
Yu (2021) <sup>120</sup>	Taiwan	HTC-RCNN (ResNet50). Decision-tree-based machine learning algorithm, XGBoost	Lymphoma	Pathologist diagnosis with WHO criteria, pathologist annotations	17 hospitals in Taiwan (names not specified)	Detect: 27 ROIs. Classify 3 fold validation from 40 WSIs	Detect: 2 ROIs. Classify: 3 fold validation from 40 WSIs	Detect: 3 ROIs. Classify: 3 fold validation from 40 WSIs	Unclear	Slide
Li (2020) <sup>121</sup>	China / USA	CNN (Inception V3)	Thyroid neoplasms	Pathologist review	Peking Union Medical College Hospital	279 WSIs	70 WSIs	259 WSIs	No	Slide
Xu (2017) <sup>122</sup>	China	CNN (AlexNet) + SVM classifier	Multiple diseases (Brain tumours, colorectal cancer)	MICCAI brain: Labels Colorectal: Pathologist review & image crops	MICCAI 2014 Brain Tumor Digital Pathology Challenge & colon cancer dataset	80 images (brain) + 359 cropped images (colon)		61 images (Brain) + 358 cropped images (Colon)	No	Patch / Tile
DiPalma (2021) <sup>123</sup>	USA	CNN (Resnet architecture but trained from scratch)	Multiple diseases (Coeliac, lung cancer, renal cancer)	RCC & Coeliac: Pathologist diagnosis, Lung: pathologist annotations	TCGA, Dartmouth-Hitchcock Medical Centre	Coeliac: 5908 tissue pieces; Lung: 239 WSIs, 2083 tissue pieces; Renal: 617 WSIs, 834 tissue pieces.	Coeliac: 1167 tissue pieces;	Coeliac: 25,284 tissue pieces; Lung: 34 WSIs, 305 tissue pieces; Renal: 265 WSIs, 364 tissue pieces.	No	Slide
Litjens (2016) <sup>124</sup>	Netherlands	CNN	Multiple diseases (Prostate cancer; Breast cancer)	Pathologist annotations / supervision, pathology reports.	3 datasets from Radboud University Medical Centre	Prostate: 100 WSIs; Breast: 98 WSIs.	Prostate: 50 WSIs; Breast: 33 WSI.	Prostate: 75 WSIs; Breast: 42 WSIs + 98 WSI consecutive set.	No	Slide
Menon (2022) <sup>125</sup>	India	ResNet-18 fully connected network (FCN)	Multiple cancer types	Slide labels	TCGA	6855 WSIs	1958 WSIs	979 WSIs	No	Patch / Tile
Noorbakhsh (2020) <sup>126</sup>	USA	CNN (InceptionV3)	Multiple cancer types	Pathologist annotations	TCGA, CPTAC.	19,470 WSIs		10,460 WSIs	Yes	Slide
Yan (2022) <sup>127</sup>	China	Contrastive clustering algorithm to train CNN encoder + recursive cluster refinement method	Multiple diseases (colorectal cancer / polyps, breast cancer)	NCT-CRC Patch classification, CAMELYON16 annotations. In-house: pathologist diagnosis	NCT-CRC dataset; Camelyon16 dataset; In-house colon polyp WSI dataset	NCT-CRC 80,000 patches; CAMELYON16 80,000 patches;	NCT-CRC 10,000 patches; CAMELYON16 10,000 patches.	NCT-CRC + In house polyp dataset: 10,000 patches + 20 patients; CAMELYON16 10,000 patches 139 WSIs	Yes	Patch / Tile
Li (2018) <sup>128</sup>	China	GoogLeNet CNN	Brain cancer	Diagnosed WSIs	Huashan Hospital, Fudan University	67 WSIs			No	Patch / Tile
Schilling (2018) <sup>129</sup>	Germany	Voting ensemble classifier (logistic regression, SVM, decision tree & random forest)	Hirsprungs disease	Pathologist diagnosis against criteria, IHC	Institute of Pathology, Friedrich-Alexander-University Erlangen Nurnberg, Germany	172 WSIs	58 WSIs	77 WSIs	No	Unclear
Mishra (2017) <sup>130</sup>	USA	CNN (LeNet & AlexNet)	Osteosarcoma	Manual annotations by senior pathologists.	Unclear	38,400 patches	12,800 patches	12,800 patches	No	Patch / Tile
Zhang (2022) <sup>131</sup>	USA	CNN (Inception V3)	Rhabdomyosarcoma	WSIs reviewed and classified by pathologist	Children's oncology group biobanking study	56 WSIs	12 WSIs	204 WSIs	Unclear	Patch / Tile

## Risk of bias and applicability

The risk of bias and applicability assessment using the tailored QUADAS-2 tool demonstrated that the majority of papers were either at high risk of bias or were unclear when assessing the risk of bias (**Figure 2**). The full breakdown of individual paper scores can be found in the supplementary materials. All 100 studies included in the systematic review demonstrated at least one area at high or unclear risk of bias, with many having multiple components at risk.

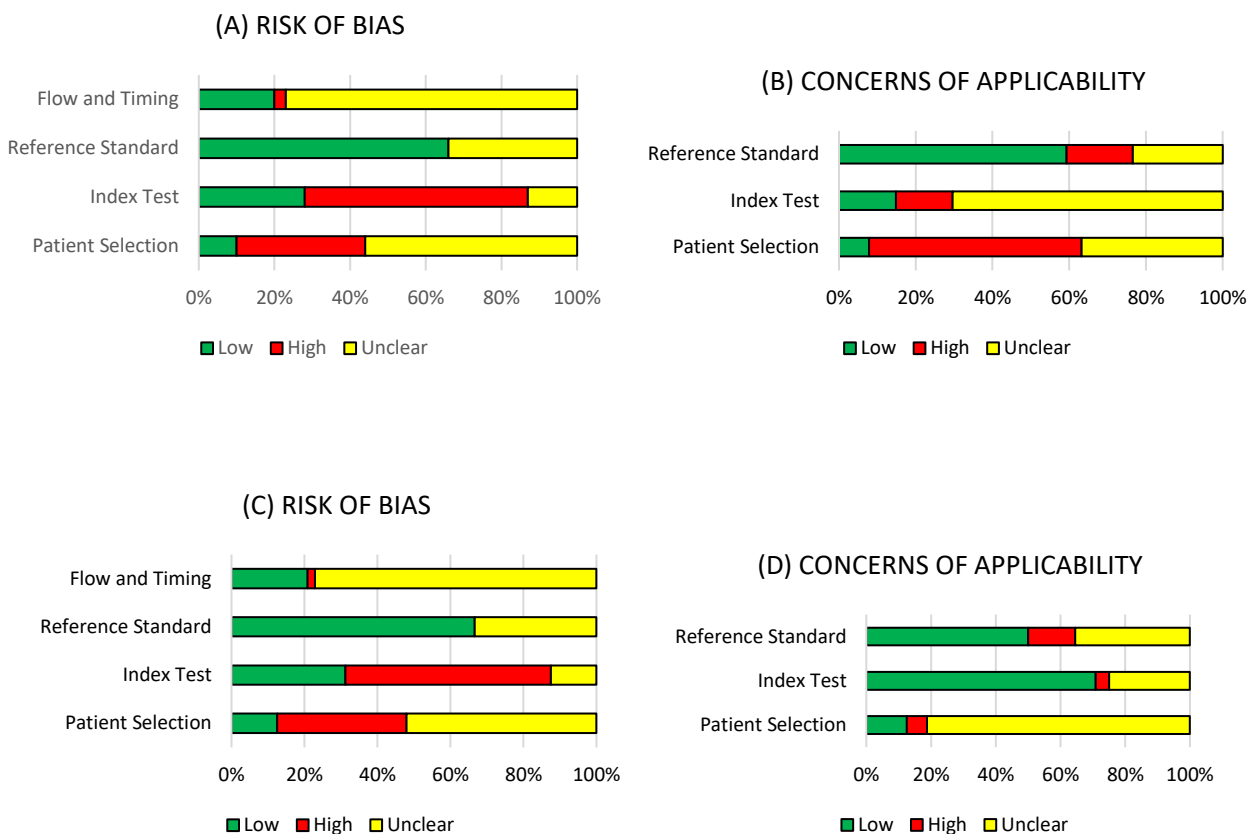


**Figure 3** – Risk of bias and concerns of applicability in summary percentages for studies included in the review. (A) & (B): Summaries for all 100 papers included in the review. (C) & (D): Summaries for 48 papers included in the meta-analysis.

Of the 48 studies included in the meta-analysis (**Figure 2C** and **Figure 2D**), 42 of 48 studies were either at high or unclear risk of bias for patient selection and 33 of 48 studies were at high or unclear risk of bias concerning the index test. The most common reasons for this included cases not being selected randomly or consecutively, or the selection method being unclear, the absence of external validation of the study's findings and it was sometimes unclear whether training and testing data were mixed. 16 of 48 studies were unclear in terms of their risk of bias for the reference standard, but no studies were considered high risk in this domain. For flow and timing, one study was at high risk but 37 of 48 studies were at unclear risk of bias.

There were concerns of applicability for many papers included in the meta-analysis with 42 of 48 studies with either unclear or high concerns for applicability in the patient selection, 14 of 48 studies with unclear or high concern for the index test and 24 of 48 studies with unclear or high concern for the reference standard. Examples for this included a lack of clarity around the selection of cases and the risk of excluding subgroups, and limited or no details given around the diagnostic criteria and pathologist involvement when describing the ground truth.

## Synthesis of results

Of the 100 studies identified for inclusion in this systematic review, 48 studies had data that could be meta-analysed. Two of the studies in the meta-analysis had available data for two different disease types,<sup>98,124</sup> meaning a total of 50 assessments included in the meta-analysis. **Figure 4** shows the forest plots for sensitivity of any AI solution applied to whole slide images. Overall, there is strong performance across studies and disease types. The mean sensitivity across all studies was 96.3% (CI 94.1-97.7) and mean specificity was 93.3% (CI 90.5-95.4), as shown in **Figure 5**.

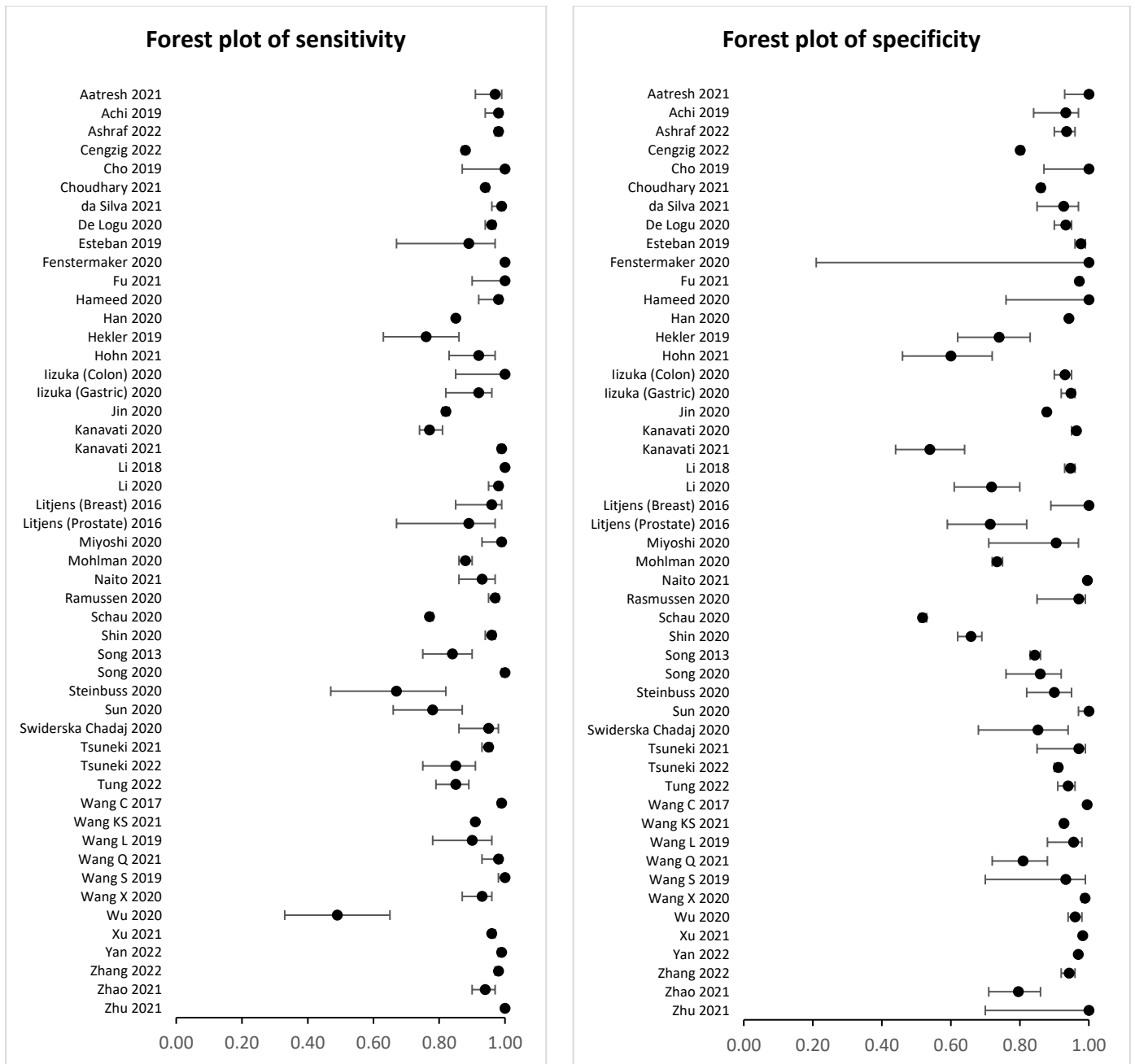


**Figure 4** – Forest plots for sensitivity and specificity in studies of all pathologies

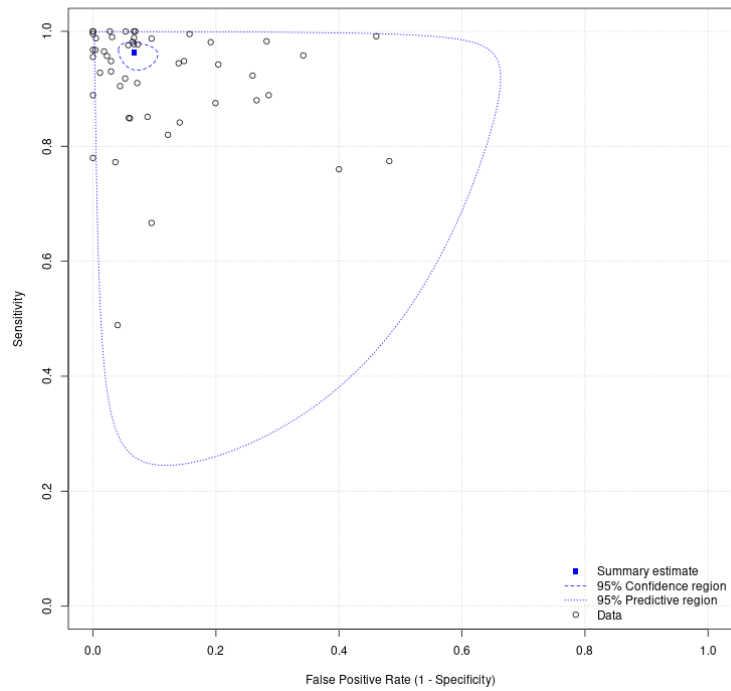


**Figure 5** – Summary receiver operating characteristic plot of AI applied to whole slide images for all disease types. 95% confidence intervals are shown around the summary estimate. The predictive region shows the area of 95% confidence in which the true sensitivity and specificity of future studies lies, whilst factoring the statistical heterogeneity of studies demonstrated in this review.

<b>Table 8. Mean performance across studies by pathological subspecialty</b>			
<b>Pathological subspecialty</b>	<b>No. studies</b>	<b>Mean sensitivity</b>	<b>Mean specificity</b>
Gastrointestinal pathology	14	93%	94%
Breast pathology	8	83%	88%
Uropathology	8	95%	96%
Hepatobiliary pathology	5	90%	87%
Dermatopathology	4	89%	81%
Cardiothoracic pathology	3	98%	76%
Haematopathology	3	95%	86%
Gynaecological pathology	2	87%	83%
Soft tissue & bone pathology	1	98%	94%
Head & neck pathology	1	98%	72%
Neuropathology	1	100%	95%

The largest subgroups of studies available for inclusion in the meta-analysis were studies of gastrointestinal pathology<sup>78,84-87,89,90,92,94,95,97,98,127</sup>, breast pathology<sup>32,33,36,37,39,46,47,124</sup> and urological pathology<sup>99,101,103,105,106,108,110,124</sup> which are shown in **Table 8**. Notably, studies of gastrointestinal pathology had a mean sensitivity of 93% and mean specificity of 94%. Similarly, studies of uropathology had mean sensitivities and specificities of 95% and 96% respectively. Studies of breast pathology had slightly lower performance at mean sensitivity of 83% and mean specificity of 88%. Results for all other disease types are also included in the meta-analysis.<sup>52,53,56,61-63,65,67,71-74,112,113,115-117,121,128,131</sup> Forest plots for these subgroups are shown in the supplementary materials. For studies that could not be included in the meta-analysis, an indication of best performance from other accuracy metrics provided is outlined in the supplementary materials.

## DISCUSSION

AI has been applied across medicine, with examples of innovation in clinical imaging, electronic health records (HER), clinical decision making, genomics, wearables, drug development and robotics to name a few.<sup>132-137</sup> The potential of AI in digital pathology has seen much recent exploration, with a growth of research in this area.<sup>138</sup> Studies have demonstrated the potential of AI in pathology for diagnosis, prognostication, treatment response and genetic mutations.<sup>4,5,7</sup> Various tools have now received regulatory approval for applications in pathology, with some examples being trialled in clinical settings.<sup>99,139</sup> Whilst these are exciting developments, ensuring that products are accurate and underpinned by robust evidence is essential for future clinical utility.

### Findings

This study sought to determine the diagnostic test accuracy of artificial intelligence solutions applied to whole slide images to diagnose disease. Overall, the meta-analysis showed that AI has a high sensitivity and specificity for diagnostic tasks across a variety of disease types in whole slide images (**Figure 4**). The performance of the models described in studies that were not included in the meta-analysis were also promising (see supplementary materials).

Subgroups of gastrointestinal pathology, breast pathology and urological pathology studies were examined in more detail, as these were the largest subsets of studies identified (see supplementary materials). The gastrointestinal subgroup included AI models for colorectal cancer<sup>84-87,98,127</sup>, gastric cancer<sup>89,90,92-95,98</sup> and gastritis<sup>97</sup>. The breast subgroup included only AI models for breast cancer applications, with Hameed et al. and Wang et al. demonstrating particularly strong sensitivity and specificity.<sup>36,46</sup> Overall results were most favourable for the subgroup of urological studies with both high mean sensitivity and specificity (**Table 8**). This subgroup included models for renal cancer<sup>108,110</sup> and prostate cancer<sup>99,101,103,105,106,124</sup>.

Of studies of other disease types included in the meta-analysis (**Figure 4**), AI models in liver cancer<sup>67</sup>, lymphoma<sup>115</sup>, melanoma<sup>61</sup>, pancreatic cancer<sup>72</sup>, brain cancer<sup>128</sup> lung cancer<sup>53</sup> and rhabdomyosarcoma<sup>131</sup> all demonstrated a high sensitivity and specificity. This emphasises the breadth of potential diagnostic tools for clinical applications with a strong performance in digital pathology.

### Limitations

It must be acknowledged that there is uncertainty in the interpretation of the diagnostic accuracy of the AI models demonstrated in these studies. There was substantial heterogeneity in the study design, metrics used to demonstrate diagnostic accuracy, size of datasets, unit of analysis (e.g. slide, patch, pixel, specimen) and the level of detail given on the process and conduct of the studies. For instance, total number of WSIs used in the studies ranged from as few as 4 WSIs to nearly 30,000 WSIs used across development and testing of an AI model.<sup>60,126</sup> All 100 papers identified for inclusion in this review had at least one area at high or uncertain risk of bias, meaning any results should be interpreted with caution. Many studies had multiple areas at risk of bias and applicability concerns (**Figure 3**).

Whilst 100 papers were identified, only 48 studies were included in the meta-analysis due to deficient reporting. Whilst the meta-analysis provided a useful indication of diagnostic accuracy across disease areas, data for true positive, false positive, false negative and true negative was frequently missing and therefore made the assessment more challenging. To address this problem, missing data was requested from authors. Where a multiclass study output was provided, this was combined into a 2x2 confusion matrix to reflect disease detection / diagnosis, however this offers a more limited indication of diagnostic accuracy. AI specific reporting guidelines for diagnostic accuracy should help to improve this problem in future.<sup>28</sup>

## Conclusions

There are many promising applications for AI models in whole slide imaging to assist the pathologist. This systematic review has outlined a favourable diagnostic accuracy for AI across multiple disease types. However, better quality study design, transparency, reporting quality and addressing substantial areas of bias is needed to improve the evidence quality in this field.

## **ACKNOWLEDGEMENTS**

Prof. Treanor, Dr McGenity, Dr Jennings and Dr Matthews are funded by the National Pathology Imaging Co-operative (NPIC). NPIC (project no. 104687) is supported by a £50m investment from the Data to Early Diagnosis and Precision Medicine strand of the Government's Industrial Strategy Challenge Fund, managed and delivered by UK Research and Innovation (UKRI).

Dr Clarke was supported by the Medical Research Council (MR/S001530/1).

The funders had no role in the study design, data collection, data analysis or writing the manuscript.

We thank the authors who kindly provided additional data for the meta-analysis.

## REFERENCES

1. Tizhoosh, H.R. & Pantanowitz, L. Artificial intelligence and digital pathology: challenges and opportunities. *J Pathol Inform* **9**, 38 (2018).
2. Pantanowitz, L., *et al.* Twenty years of digital pathology: an overview of the road travelled, what is on the horizon, and the emergence of vendor-neutral archives. *J Pathol Inform* **9**, 40 (2018).
3. Colling, R., *et al.* Artificial intelligence in digital pathology: a roadmap to routine use in clinical practice. *The Journal of pathology* **249**, 143-150 (2019).
4. Acs, B., Rantalainen, M. & Hartman, J. Artificial intelligence as the next step towards precision pathology. *J Intern Med* **288**, 62-81 (2020).
5. Srinidhi, C.L., Ciga, O. & Martel, A.L. Deep neural network models for computational histopathology: A survey. *Medical Image Analysis* **67**, 101813 (2021).
6. Niazi, M.K.K., Parwani, A.V. & Gurcan, M.N. Digital pathology and artificial intelligence. *The lancet oncology* **20**, e253-e261 (2019).
7. Bera, K., Schalper, K.A., Rimm, D.L., Velcheti, V. & Madabhushi, A. Artificial intelligence in digital pathology—new tools for diagnosis and precision oncology. *Nature reviews Clinical oncology* **16**, 703-715 (2019).
8. Baxi, V., Edwards, R., Montalto, M. & Saha, S. Digital pathology and artificial intelligence in translational medicine and clinical practice. *Modern Pathology* **35**, 23-32 (2022).
9. Ehteshami Bejnordi, B., *et al.* Diagnostic Assessment of Deep Learning Algorithms for Detection of Lymph Node Metastases in Women With Breast Cancer. *JAMA* **318**, 2199-2210 (2017).
10. Lu, M.Y., *et al.* AI-based pathology predicts origins for cancers of unknown primary. *Nature* **594**, 106-110 (2021).
11. Wulczyn, E., *et al.* Interpretable survival prediction for colorectal cancer using deep learning. *NPJ digital medicine* **4**, 71 (2021).
12. Fu, Y., *et al.* Pan-cancer computational histopathology reveals mutations, tumor composition and prognosis. *Nature cancer* **1**, 800-810 (2020).
13. Thakur, N., Yoon, H. & Chong, Y. Current trends of artificial intelligence for colorectal cancer pathology image analysis: a systematic review. *Cancers* **12**, 1884 (2020).
14. Krithiga, R. & Geetha, P. Breast cancer detection, segmentation and classification on histopathology images analysis: a systematic review. *Archives of Computational Methods in Engineering* **28**, 2607-2619 (2021).
15. Allaume, P., *et al.* Artificial Intelligence-Based Opportunities in Liver Pathology—A Systematic Review. *Diagnostics* **13**, 1799 (2023).
16. Clarke, E.L., Wade, R.G., Magee, D., Newton-Bishop, J. & Treanor, D. Image analysis of cutaneous melanoma histology: a systematic review and meta-analysis. *Scientific Reports* **13**, 4774 (2023).
17. Girolami, I., *et al.* Artificial intelligence applications for pre-implantation kidney biopsy pathology practice: a systematic review. *Journal of Nephrology* **35**, 1801-1808 (2022).
18. Rodriguez, J.P.M., *et al.* Artificial intelligence as a tool for diagnosis in digital pathology whole slide images: a systematic review. *J Pathol Inform*, 100138 (2022).
19. Parikh, R.B., Teeple, S. & Navathe, A.S. Addressing bias in artificial intelligence in health care. *Jama* **322**, 2377-2378 (2019).
20. Varoquaux, G. & Cheplygina, V. Machine learning for medical imaging: methodological failures and recommendations for the future. *NPJ digital medicine* **5**, 48 (2022).
21. Nagendran, M., *et al.* Artificial intelligence versus clinicians: systematic review of design, reporting standards, and claims of deep learning studies. *BMJ* **368**, m689 (2020).
22. The Royal College of Pathologists. Meeting pathology demand - Histopathology workforce census 2017/2018. (The Royal College of Pathologists, London, 2018).
23. The Royal College of Pathologists. Position statement from the Royal College of Pathologists (RCPATH) on Digital Pathology and Artificial Intelligence (AI). (London, UK, 2023).
24. University of Leeds. Leeds Virtual Pathology. Vol. 2022 (Leeds, UK, 2022).
25. Salameh, J.-P., *et al.* Preferred reporting items for systematic review and meta-analysis of diagnostic test accuracy studies (PRISMA-DTA): explanation, elaboration, and checklist. *bmj* **370**(2020).
26. Sounderajah, V., *et al.* A quality assessment tool for artificial intelligence-centered diagnostic test accuracy studies: QUADAS-AI. *Nature medicine* **27**, 1663-1665 (2021).
27. Whiting, P.F., *et al.* QUADAS-2: a revised tool for the quality assessment of diagnostic accuracy studies. *Annals of internal medicine* **155**, 529-536 (2011).
28. Sounderajah, V., *et al.* Developing a reporting guideline for artificial intelligence-centred diagnostic test accuracy studies: the STARD-AI protocol. *BMJ open* **11**, e047709 (2021).

29. McGuinness, L.A. & Higgins, J.P. Risk-of-bias VISualization (robvis): an R package and Shiny web app for visualizing risk-of-bias assessments. *Research synthesis methods* **12**, 55-61 (2021).
30. Patel, A., Cooper, N., Freeman, S. & Sutton, A. Graphical enhancements to summary receiver operating characteristic plots to facilitate the analysis and reporting of meta-analysis of diagnostic test accuracy data. *Research synthesis methods* **12**, 34-44 (2021).
31. Haddaway, N.R., Page, M.J., Pritchard, C.C. & McGuinness, L.A. PRISMA2020: An R package and Shiny app for producing PRISMA 2020-compliant flow diagrams, with interactivity for optimised digital transparency and Open Synthesis. *Campbell Systematic Reviews* **18**, e1230 (2022).
32. Cengiz, E., Kelek, M.M., Oğuz, Y. & Yılmaz, C. Classification of breast cancer with deep learning from noisy images using wavelet transform. *Biomed Tech (Berl)* **67**, 143-150 (2022).
33. Choudhary, T., Mishra, V., Goswami, A. & Sarangapani, J. A transfer learning with structured filter pruning approach for improved breast cancer classification on point-of-care devices. *Comput Biol Med* **134**, 104432 (2021).
34. Cruz-Roa, A., *et al.* High-throughput adaptive sampling for whole-slide histopathology image analysis (HASHI) via convolutional neural networks: Application to invasive breast cancer detection. *PLoS One* **13**, e0196828 (2018).
35. Cruz-Roa, A., *et al.* Accurate and reproducible invasive breast cancer detection in whole-slide images: A Deep Learning approach for quantifying tumor extent. *Sci Rep* **7**, 46450 (2017).
36. Hameed, Z., Zahia, S., Garcia-Zapirain, B., Javier Aguirre, J. & María Vanegas, A. Breast Cancer Histopathology Image Classification Using an Ensemble of Deep Learning Models. *Sensors (Basel)* **20**(2020).
37. Jin, Y.W., Jia, S., Ashraf, A.B. & Hu, P. Integrative data augmentation with u-net segmentation masks improves detection of lymph node metastases in breast cancer patients. *Cancers* **12**, 1-13 (2020).
38. Johnny, A. & Madhusoodanan, K.N. Dynamic Learning Rate in Deep CNN Model for Metastasis Detection and Classification of Histopathology Images. *Comput Math Methods Med* **2021**, 5557168 (2021).
39. Kanavati, F., Ichihara, S. & Tsuneki, M. A deep learning model for breast ductal carcinoma in situ classification in whole slide images. *Virchows Arch* **480**, 1009-1022 (2022).
40. Khalil, M.A., Lee, Y.C., Lien, H.C., Jeng, Y.M. & Wang, C.W. Fast Segmentation of Metastatic Foci in H&E Whole-Slide Images for Breast Cancer Diagnosis. *Diagnostics* **12**, 990 (2022).
41. Lin, H., *et al.* Fast ScanNet: Fast and Dense Analysis of Multi-Gigapixel Whole-Slide Images for Cancer Metastasis Detection. *IEEE Trans Med Imaging* **38**, 1948-1958 (2019).
42. Roy, S.D., Das, S., Kar, D., Schwenker, F. & Sarkar, R. Computer Aided Breast Cancer Detection Using Ensembling of Texture and Statistical Image Features. *Sensors (Basel)* **21**(2021).
43. Sadeghi, M., *et al.* Feedback-based Self-improving CNN Algorithm for Breast Cancer Lymph Node Metastasis Detection in Real Clinical Environment. *Annu Int Conf IEEE Eng Med Biol Soc* **2019**, 7212-7215 (2019).
44. Steiner, D.F., *et al.* Impact of Deep Learning Assistance on the Histopathologic Review of Lymph Nodes for Metastatic Breast Cancer. *Am J Surg Pathol* **42**, 1636-1646 (2018).
45. Valkonen, M., *et al.* Metastasis detection from whole slide images using local features and random forests. *Cytometry A* **91**, 555-565 (2017).
46. Wang, Q., Zou, Y., Zhang, J. & Liu, B. Second-order multi-instance learning model for whole slide image classification. *Phys Med Biol* **66**(2021).
47. Wu, W., *et al.* MLCD: A Unified Software Package for Cancer Diagnosis. *JCO Clin Cancer Inform* **4**, 290-298 (2020).
48. Chen, C.L., *et al.* An annotation-free whole-slide training approach to pathological classification of lung cancer types using deep learning. *Nat Commun* **12**, 1193 (2021).
49. Yang, H., *et al.* A whole-slide image (WSI)-based immunohistochemical feature prediction system improves the subtyping of lung cancer. *Lung Cancer* **165**, 18-27 (2022).
50. Coudray, N., *et al.* Classification and mutation prediction from non-small cell lung cancer histopathology images using deep learning. *Nat Med* **24**, 1559-1567 (2018).
51. Dehkharghanian, T., *et al.* Selection, Visualization, and Interpretation of Deep Features in Lung Adenocarcinoma and Squamous Cell Carcinoma. *Am J Pathol* **191**, 2172-2183 (2021).
52. Kanavati, F., *et al.* Weakly-supervised learning for lung carcinoma classification using deep learning. *Sci Rep* **10**, 9297 (2020).
53. Wang, X., *et al.* Weakly Supervised Deep Learning for Whole Slide Lung Cancer Image Analysis. *IEEE Trans Cybern* **50**, 3950-3962 (2020).
54. Wei, J.W., *et al.* Pathologist-level classification of histologic patterns on resected lung adenocarcinoma slides with deep neural networks. *Sci Rep* **9**, 3358 (2019).

55. Yang, H., *et al.* Deep learning-based six-type classifier for lung cancer and mimics from histopathological whole slide images: a retrospective study. *BMC Med* **19**, 80 (2021).
56. Zhao, L., *et al.* Lung cancer subtype classification using histopathological images based on weakly supervised multi-instance learning. *Phys Med Biol* **66**(2021).
57. Zheng, Y., *et al.* A Graph-Transformer for Whole Slide Image Classification. *IEEE Transactions on Medical Imaging* **41**, 3003-3015 (2022).
58. Uegami, W., *et al.* MIXTURE of human expertise and deep learning-developing an explainable model for predicting pathological diagnosis and survival in patients with interstitial lung disease. *Mod Pathol* **35**, 1083-1091 (2022).
59. Kimeswenger, S., *et al.* Artificial neural networks and pathologists recognize basal cell carcinomas based on different histological patterns. *Mod Pathol* **34**, 895-903 (2021).
60. Alheejawi, S., Berendt, R., Jha, N., Maity, S.P. & Mandal, M. Detection of malignant melanoma in H&E-stained images using deep learning techniques. *Tissue Cell* **73**, 101659 (2021).
61. De Logu, F., *et al.* Recognition of Cutaneous Melanoma on Digitized Histopathological Slides via Artificial Intelligence Algorithm. *Frontiers in Oncology* **10**, 1559 (2020).
62. Hekler, A., *et al.* Deep learning outperformed 11 pathologists in the classification of histopathological melanoma images. *Eur J Cancer* **118**, 91-96 (2019).
63. Höhn, J., *et al.* Combining CNN-based histologic whole slide image analysis and patient data to improve skin cancer classification. *European Journal of Cancer* **149**, 94-101 (2021).
64. Li, T., *et al.* Automated Diagnosis and Localization of Melanoma from Skin Histopathology Slides Using Deep Learning: A Multicenter Study. *J Healthc Eng* **2021**, 5972962 (2021).
65. Wang, L., *et al.* Automated identification of malignancy in whole-slide pathological images: identification of eyelid malignant melanoma in gigapixel pathological slides using deep learning. *Br J Ophthalmol* **104**, 318-323 (2020).
66. Del Amor, R., *et al.* An attention-based weakly supervised framework for spitzoid melanocytic lesion diagnosis in whole slide images. *Artif Intell Med* **121**, 102197 (2021).
67. Aatresh, A.A., Alabhya, K., Lal, S., Kini, J. & Saxena, P.U.P. LiverNet: efficient and robust deep learning model for automatic diagnosis of sub-types of liver hepatocellular carcinoma cancer from H&E stained liver histopathology images. *Int J Comput Assist Radiol Surg* **16**, 1549-1563 (2021).
68. Chen, M., *et al.* Classification and mutation prediction based on histopathology H&E images in liver cancer using deep learning. *NPJ precision oncology* **4**, 1-7 (2020).
69. Kiani, A., *et al.* Impact of a deep learning assistant on the histopathologic classification of liver cancer. Vol. 3 23 (Nature Research (E-mail: subscriptions@nature.com), 2020).
70. Yang, T.L., *et al.* Pathologic liver tumor detection using feature aligned multi-scale convolutional network. *Artif Intell Med* **125**, 102244 (2022).
71. Schau, G.F., *et al.* Predicting primary site of secondary liver cancer with a neural estimator of metastatic origin. *Journal of Medical Imaging* **7**, 012706 (2020).
72. Fu, H., *et al.* Automatic Pancreatic Ductal Adenocarcinoma Detection in Whole Slide Images Using Deep Convolutional Neural Networks. *Frontiers in Oncology* **11**, 665929 (2021).
73. Naito, Y., *et al.* A deep learning model to detect pancreatic ductal adenocarcinoma on endoscopic ultrasound-guided fine-needle biopsy. *Sci Rep* **11**, 8454 (2021).
74. Song, J.W., Lee, J.H., Choi, J.H. & Chun, S.J. Automatic differential diagnosis of pancreatic serous and mucinous cystadenomas based on morphological features. *Comput Biol Med* **43**, 1-15 (2013).
75. Sali, R., *et al.* Deep learning for whole-slide tissue histopathology classification: A comparative study in the identification of dysplastic and non-dysplastic barrett's esophagus. *Journal of Personalized Medicine* **10**, 1-16 (2020).
76. Syed, S., *et al.* Artificial Intelligence-based Analytics for Diagnosis of Small Bowel Enteropathies and Black Box Feature Detection. *J Pediatr Gastroenterol Nutr* **72**, 833-841 (2021).
77. Nasir-Moin, M., *et al.* Evaluation of an Artificial Intelligence-Augmented Digital System for Histologic Classification of Colorectal Polyps. *JAMA Netw Open* **4**, e2135271 (2021).
78. Song, Z., *et al.* Automatic deep learning-based colorectal adenoma detection system and its similarities with pathologists. *BMJ Open* **10**, e036423 (2020).
79. Wei, J.W., *et al.* Evaluation of a Deep Neural Network for Automated Classification of Colorectal Polyps on Histopathologic Slides. *JAMA Netw Open* **3**, e203398 (2020).
80. Feng, R., *et al.* A Deep Learning Approach for Colonoscopy Pathology WSI Analysis: Accurate Segmentation and Classification. *IEEE Journal of Biomedical and Health Informatics* **25**, 3700-3708 (2021).
81. Haryanto, T., Suhartanto, H., Arymurthy, A.M. & Kusmardi, K. Conditional sliding windows: An approach for handling data limitation in colorectal histopathology image classification. *Informatics in Medicine Unlocked* **23**, 100565 (2021).

82. Sabol, P., *et al.* Explainable classifier for improving the accountability in decision-making for colorectal cancer diagnosis from histopathological images. *J Biomed Inform* **109**, 103523 (2020).
83. Schrammen, P.L., *et al.* Weakly supervised annotation-free cancer detection and prediction of genotype in routine histopathology. *J Pathol* **256**, 50-60 (2022).
84. Tsuneki, M. & Kanavati, F. Deep learning models for poorly differentiated colorectal adenocarcinoma classification in whole slide images using transfer learning. *Diagnostics* **11**, 2074 (2021).
85. Wang, K.S., *et al.* Accurate diagnosis of colorectal cancer based on histopathology images using artificial intelligence. *BMC Medicine* **19**, 76 (2021).
86. Wang, C., Shi, J., Zhang, Q. & Ying, S. Histopathological image classification with bilinear convolutional neural networks. in *2017 39th Annual International Conference of the IEEE Engineering in Medicine and Biology Society (EMBC)* 4050-4053 (2017).
87. Xu, Y., Jiang, L., Huang, S., Liu, Z. & Zhang, J. Dual resolution deep learning network with self-attention mechanism for classification and localisation of colorectal cancer in histopathological images. *Journal of clinical pathology* (2022).
88. Zhou, C., *et al.* Histopathology classification and localization of colorectal cancer using global labels by weakly supervised deep learning. *Computerized Medical Imaging and Graphics* **88**, 101861 (2021).
89. Ashraf, M., Robles, W.R.Q., Kim, M., Ko, Y.S. & Yi, M.Y. A loss-based patch label denoising method for improving whole-slide image analysis using a convolutional neural network. *Scientific reports* **12**, 1392 (2022).
90. Cho, K.O., Lee, S.H. & Jang, H.J. Feasibility of fully automated classification of whole slide images based on deep learning. *Korean Journal of Physiology and Pharmacology* **24**, 89-99 (2020).
91. Ma, B., *et al.* Artificial Intelligence-Based Multiclass Classification of Benign or Malignant Mucosal Lesions of the Stomach. *Frontiers in Pharmacology* **11**, 572372 (2020).
92. Rasmussen, S., Arnason, T. & Huang, W.Y. Deep learning for computer assisted diagnosis of hereditary diffuse gastric cancer. *Modern pathology* **33**, 755-756 (2020).
93. Song, Z., *et al.* Clinically applicable histopathological diagnosis system for gastric cancer detection using deep learning. *Nat Commun* **11**, 4294 (2020).
94. Tung, C.L., *et al.* Identifying pathological slices of gastric cancer via deep learning. *J Formos Med Assoc* **121**, 2457-2464 (2022).
95. Wang, S., *et al.* RMDL: Recalibrated multi-instance deep learning for whole slide gastric image classification. *Med Image Anal* **58**, 101549 (2019).
96. Ba, W., *et al.* Histopathological Diagnosis System for Gastritis Using Deep Learning Algorithm. *Chin Med Sci J* **36**, 204-209 (2021).
97. Steinbuss, G., Kriegsmann, K. & Kriegsmann, M. Identification of Gastritis Subtypes by Convolutional Neuronal Networks on Histological Images of Antrum and Corpus Biopsies. *Int J Mol Sci* **21**(2020).
98. Iizuka, O., *et al.* Deep Learning Models for Histopathological Classification of Gastric and Colonic Epithelial Tumours. *Sci Rep* **10**, 1504 (2020).
99. da Silva, L.M., *et al.* Independent real-world application of a clinical-grade automated prostate cancer detection system. *Journal of Pathology* **254**, 147-158 (2021).
100. Duran-Lopez, L., *et al.* Wide & Deep neural network model for patch aggregation in CNN-based prostate cancer detection systems. *Comput Biol Med* **136**, 104743 (2021).
101. Esteban, A.E., *et al.* A new optical density granulometry-based descriptor for the classification of prostate histological images using shallow and deep Gaussian processes. *Computer Methods and Programs in Biomedicine* **178**, 303-317 (2019).
102. Han, W., *et al.* Histologic tissue components provide major cues for machine learning-based prostate cancer detection and grading on prostatectomy specimens. *Sci Rep* **10**, 9911 (2020).
103. Han, W., *et al.* Automatic cancer detection on digital histopathology images of mid-gland radical prostatectomy specimens. *Journal of Medical Imaging* **7**, 047501 (2020).
104. Huang, W., *et al.* Development and Validation of an Artificial Intelligence-Powered Platform for Prostate Cancer Grading and Quantification. *JAMA Netw Open* **4**, e2132554 (2021).
105. Swiderska-Chadaj, Z., *et al.* Impact of rescanning and normalization on convolutional neural network performance in multi-center, whole-slide classification of prostate cancer. *Sci Rep* **10**, 14398 (2020).
106. Tsuneki, M., Abe, M. & Kanavati, F. A Deep Learning Model for Prostate Adenocarcinoma Classification in Needle Biopsy Whole-Slide Images Using Transfer Learning. *Diagnostics* **12**, 768 (2022).

107. Abdeltawab, H., *et al.* A pyramidal deep learning pipeline for kidney whole-slide histology images classification. *Sci Rep* **11**, 20189 (2021).
108. Fenstermaker, M., Tomlins, S.A., Singh, K., Wiens, J. & Morgan, T.M. Development and Validation of a Deep-learning Model to Assist With Renal Cell Carcinoma Histopathologic Interpretation. *Urology* **144**, 152-157 (2020).
109. Tabibu, S., Vinod, P.K. & Jawahar, C.V. Pan-Renal Cell Carcinoma classification and survival prediction from histopathology images using deep learning. *Sci Rep* **9**, 10509 (2019).
110. Zhu, M., *et al.* Development and evaluation of a deep neural network for histologic classification of renal cell carcinoma on biopsy and surgical resection slides. *Sci Rep* **11**, 7080 (2021).
111. BenTaieb, A., Li-Chang, H., Huntsman, D. & Hamarneh, G. A structured latent model for ovarian carcinoma subtyping from histopathology slides. *Med Image Anal* **39**, 194-205 (2017).
112. Shin, S.J., *et al.* Style transfer strategy for developing a generalizable deep learning application in digital pathology. *Comput Methods Programs Biomed* **198**, 105815 (2021).
113. Sun, H., Zeng, X., Xu, T., Peng, G. & Ma, Y. Computer-Aided Diagnosis in Histopathological Images of the Endometrium Using a Convolutional Neural Network and Attention Mechanisms. *IEEE J Biomed Health Inform* **24**, 1664-1676 (2020).
114. Yu, K.H., *et al.* Deciphering serous ovarian carcinoma histopathology and platinum response by convolutional neural networks. *BMC Med* **18**, 236 (2020).
115. Achi, H.E., *et al.* Automated Diagnosis of Lymphoma with Digital Pathology Images Using Deep Learning. *Ann Clin Lab Sci* **49**, 153-160 (2019).
116. Miyoshi, H., *et al.* Deep learning shows the capability of high-level computer-aided diagnosis in malignant lymphoma. *Lab Invest* **100**, 1300-1310 (2020).
117. Mohlman, J., Leventhal, S., Pascucci, V. & Salama, M. Improving augmented human intelligence to distinguish burkitt lymphoma from diffuse large B-cell lymphoma cases. *American journal of clinical pathology* **152**, S122- (2019).
118. Syrykh, C., *et al.* Accurate diagnosis of lymphoma on whole-slide histopathology images using deep learning. *NPJ digital medicine* **3**, 63 (2020).
119. Yu, K.H., *et al.* Classifying non-small cell lung cancer types and transcriptomic subtypes using convolutional neural networks. *J Am Med Inform Assoc* **27**, 757-769 (2020).
120. Yu, W.H., Li, C.H., Wang, R.C., Yeh, C.Y. & Chuang, S.S. Machine learning based on morphological features enables classification of primary intestinal t-cell lymphomas. *Cancers* **13**, 5463 (2021).
121. Li, Y., *et al.* Rule-based automatic diagnosis of thyroid nodules from intraoperative frozen sections using deep learning. *Artif Intell Med* **108**, 101918 (2020).
122. Xu, Y., *et al.* Large scale tissue histopathology image classification, segmentation, and visualization via deep convolutional activation features. *BMC bioinformatics* **18**, 281 (2017).
123. DiPalma, J., Suriawinata, A.A., Tafe, L.J., Torresani, L. & Hassanpour, S. Resolution-based distillation for efficient histology image classification. *Artif Intell Med* **119**, 102136 (2021).
124. Litjens, G., *et al.* Deep learning as a tool for increased accuracy and efficiency of histopathological diagnosis. *Sci Rep* **6**, 26286 (2016).
125. Menon, A., Singh, P., Vinod, P.K. & Jawahar, C.V. Exploring Histological Similarities Across Cancers From a Deep Learning Perspective. *Frontiers in Oncology* **12**, 842759 (2022).
126. Noorbakhsh, J., *et al.* Deep learning-based cross-classifications reveal conserved spatial behaviors within tumor histological images. *Nat Commun* **11**, 6367 (2020).
127. Yan, J., Chen, H., Li, X. & Yao, J. Deep contrastive learning based tissue clustering for annotation-free histopathology image analysis. *Comput Med Imaging Graph* **97**, 102053 (2022).
128. Li, X., Cheng, H., Wang, Y. & Yu, J. Histological subtype classification of gliomas in digital pathology images based on deep learning approach. *Journal of Medical Imaging and Health Informatics* **8**, 1422-1427 (2018).
129. Schilling, F., *et al.* Digital pathology imaging and computer-aided diagnostics as a novel tool for standardization of evaluation of aganglionic megacolon (Hirschsprung disease) histopathology. *Cell Tissue Res* **375**, 371-381 (2019).
130. Mishra, R., Daescu, O., Leavey, P., Rakheja, D. & Sengupta, A. Convolutional Neural Network for Histopathological Analysis of Osteosarcoma. *J Comput Biol* **25**, 313-325 (2018).
131. Zhang, X., *et al.* Deep Learning of Rhabdomyosarcoma Pathology Images for Classification and Survival Outcome Prediction. *Am J Pathol* **192**, 917-925 (2022).
132. Aggarwal, R., *et al.* Diagnostic accuracy of deep learning in medical imaging: A systematic review and meta-analysis. *NPJ digital medicine* **4**, 1-23 (2021).

133. Xiao, C., Choi, E. & Sun, J. Opportunities and challenges in developing deep learning models using electronic health records data: a systematic review. *Journal of the American Medical Informatics Association* **25**, 1419-1428 (2018).
134. Loftus, T.J., *et al.* Artificial intelligence and surgical decision-making. *JAMA surgery* **155**, 148-158 (2020).
135. Zou, J., *et al.* A primer on deep learning in genomics. *Nature genetics* **51**, 12-18 (2019).
136. Zhang, S., *et al.* Deep learning in human activity recognition with wearable sensors: A review on advances. *Sensors* **22**, 1476 (2022).
137. Chen, H., Engkvist, O., Wang, Y., Olivecrona, M. & Blaschke, T. The rise of deep learning in drug discovery. *Drug discovery today* **23**, 1241-1250 (2018).
138. Ailia, M.J., *et al.* Current trend of artificial intelligence patents in digital pathology: a systematic evaluation of the patent landscape. *Cancers* **14**, 2400 (2022).
139. Pantanowitz, L., *et al.* An artificial intelligence algorithm for prostate cancer diagnosis in whole slide images of core needle biopsies: a blinded clinical validation and deployment study. *The Lancet Digital Health* **2**, e407-e416 (2020).



## Supplementary materials

### Contents

<b>S1 – Search strategy of three databases (PubMed, EMBASE &amp; CENTRAL)</b>	<b>2</b>
<b>S2 – Screening tools for inclusion of articles</b>	<b>3</b>
S2a: Screening tool for abstracts	3
S2b: Screening tool for full text articles	3
<b>S3 – QUADAS-2 tool tailored for this review</b>	<b>4</b>
<b>S4 – Individual paper scores for QUADAS-2 assessment</b>	<b>5</b>
<b>S5 – Other accuracy / performance metrics for papers not included in the meta-analysis</b>	<b>7</b>
<b>S6 – Meta analysis: additional data &amp; source of data</b>	<b>8</b>
<b>S7 – Supplementary forest plots of sensitivity and specificity for subgroups</b>	<b>9</b>
S7a – Forest plots for sensitivity and specificity in studies of gastrointestinal pathology	9
S7b – Forest plots for sensitivity and specificity in studies of breast pathology	9
S7c – Forest plots for sensitivity and specificity in studies of urological pathology	9
S7d – Forest plots for sensitivity and specificity in studies of other pathologies	10
<b>S8 – Further details of study characteristics</b>	<b>11</b>

## S1 – Search strategy of three databases (PubMed, EMBASE & CENTRAL)

### Pubmed

#### Limits (Humans, English)

1	digital pathol*.ti,ab.	961
2	whole slide image.ti,ab.	176
3	histopathol*.ti,ab.	132,723
4	artificial intelligence.ti,ab.	12,011
5	deep learning.ti,ab.	14,760
6	machine learning.ti,ab.	31,756
7	neural network.ti,ab.	21,974
8	computer vision.ti,ab.	2,141
9	support vector machine.ti,ab.	8,911
10	#1 OR #2 OR #3	133,553
11	#4 OR #5 OR #6 OR #7 OR #8 OR #9	70,047
12	#10 AND #11	1,279

### Embase Classic+Embase

1	digital pathol*.ti,ab.	1952
2	whole slide image.ti,ab.	408
3	histopathol*.ti,ab.	370,508
4	artificial intelligence.ti,ab.	23,908
5	deep learning.ti,ab.	31,614
6	machine learning.ti,ab.	67,418
7	neural network.ti,ab.	59,436
8	computer vision.ti,ab.	5,963
9	support vector machine.ti,ab.	19,875
10	1 or 2 or 3	372,380
11	4 or 5 or 6 or 7 or 8 or 9	166,702
12	10 and 11	2,628
13	limit 12 to (human and english language and (embase or medline))	1,537

### CENTRAL

ID	Search Hits	
#1	"digital pathol**"	0
#2	"whole slide image"	14
#3	histopathol*	10,595
#4	"artificial intelligence"	1,141
#5	"deep learning"	729
#6	"machine learning"	1,904
#7	"neural network"	1,148
#8	"computer vision"	116
#9	"support vector machine"	376
#10	#1 OR #2 OR #3	10,603
#11	#4 OR #5 OR #6 OR #7 OR #8 OR #9	4,135
#12	#10 AND #11	180
#13	#12 in Trials	160

## S2 – Screening tools for inclusion of articles

### S2a: Screening tool for abstracts

1. Is this article an original research paper? (i.e. not a review, conference abstract, commentary etc.)	No = Reject Yes = Next question
2. Is education the primary focus of the article?	Yes = Reject No = Next question
3. Is this article examining whole slide imaging? (i.e. not other imaging modalities e.g. other pathology imaging technologies, radiological imaging, endoscopy etc.)	No = Reject Yes = Next question
4. Is this article examining a surgical pathology / histopathology problem(s)? (i.e. not cytology, autopsy, toxicology, forensics, descriptions of new systems or collaborations)	No = Reject Yes = Next question
5. Is this article examining artificial intelligence for whole slide imaging? (i.e. not manual annotation etc.)	No = Reject Yes = Next question
6. Is this study examining diagnosis of a disease? (i.e. not determining only prognosis, treatment response, molecular status etc or focused on a purely quality / technical issue for WSI))	No = Reject Yes = Next question
7. Is this study measuring diagnostic accuracy? (i.e. referring to accuracy or including accuracy statistics)	No = Reject Yes = Next question
8. Is this a study of humans? (i.e. not an animal based study)	No = Reject Yes = Next question
9. Is this study written in English?	No = Reject Yes = Accept

### S2b: Screening tool for full text articles

1. Is this article an original research paper?	No = Reject Yes = Next question
2. Is education the primary focus of the article?	Yes = Reject No = Next question
3. Is this article examining whole slide imaging? (not other modalities and not combined with other modalities in the analysis)	No = Reject Yes = Next question
4. Is this article examining a surgical pathology / histopathology problem(s)?	No = Reject Yes = Next question
5. Is this article examining artificial intelligence for whole slide imaging?	No = Reject Yes = Next question
6. Is this study examining diagnosis of a disease? (detection of disease or classification of disease subtypes only)	No = Reject Yes = Next question
7. Is this study measuring diagnostic accuracy?	No = Reject Yes = Next question
8. Is this a study of humans?	No = Reject Yes = Next question
9. Is this study written in English?	No = Reject Yes = Accept
10. Does the ground truth use or imply use of human pathologist using H&E or IHC?	No = Reject Yes = Accept
11. Does the article describe a grand challenge exercise with models from multiple authors? (Rather than diagnostic accuracy study from one group)	Yes = Reject No = Accept

## S3 – QUADAS-2 tool tailored for this review

### Appendix – Adapted QUADAS2 tool

#### Domain 1: Patient Selection

##### *Risk of Bias (describe methods of patient selection)*

###### Signaling questions

- Was a consecutive or random sample of cases used in the test set(s)? Yes/No/Unclear
- Did the study avoid inappropriate exclusions? (I.e. excluding all artefacts or excluding cases that were difficult to diagnose) Yes/No/Unclear

##### **QUESTION 1 – Could the selection of patients have introduced bias? RISK: LOW/HIGH/UNCLEAR**

Low risk (1) if all the answers to signalling questions were 'yes'

High risk (2) if any of the answers to signalling questions were 'no'

Unclear (3) if answer to signalling questions was 'unclear'

##### *Concerns regarding applicability (describe included patients)*

##### **QUESTION 2 – Is there a concern that the included patients do not match the review question? CONCERN: LOW/HIGH/UNCLEAR**

Low risk (1) if cases were selected from a given condition, without excluding subgroups

High risk (2) if subgroups of cases with a given condition were excluded, not reflecting the full case mix

Unclear (3) if it is not clear how cases were selected

#### Domain 2: Index Test(s)

##### *Risk of bias (describe the index test and how it was conducted and interpreted)*

###### Signaling questions

- Were the reported performance results from test data that was independent of the training data? Yes/No/Unclear
- Was the index test tested on an external independent test set? Yes/No/Unclear
- Was the same image analysis performed on all the cases? Yes/No/Unclear
- Were all test cases used in the analysis? Yes/No/Unclear

##### **QUESTION 3 – Could the conduct or interpretation of the index test have introduced bias? RISK: LOW/HIGH/UNCLEAR**

Low risk (1) if all the answers to signalling questions were 'yes'

High risk (2) if any of the answers to signalling questions were 'no'

Unclear (3) if answer to signalling questions was 'unclear'

##### *Concerns regarding applicability*

##### **QUESTION 4 – Is there a concern that the index test, its conduct, or interpretation differ from the review question? CONCERN: LOW/HIGH/UNCLEAR**

Low risk (1) if there is no concern that the index test, its conduct or interpretation differ from the review question

High risk (2) if there is concern of either the index test, its conduct or interpretation differing from the review question

Unclear (3) if it is not clear if the index test, its conduct or interpretation differ from the review question.

#### Domain 3: Reference Standard

##### *Risk of bias (describe the reference standard and how it was conducted and interpreted)*

###### Signaling questions

- Is the reference standard likely to correctly classify the target condition? Yes/No/Unclear
- Were the reference standard results interpreted without knowledge of the results of the index test? Yes/No/Unclear

##### **QUESTION 5 – Could the reference standard, its conduct, or its interpretation have introduced bias? RISK: LOW/HIGH/UNCLEAR**

Low risk (1) if the answers to both signalling questions were 'yes'

High risk (2) if the answers to either signalling questions were 'no'

Unclear (3) if answer to either signalling questions was 'unclear'

##### *Concerns regarding applicability*

##### **QUESTION 6 – Is there concern that the target condition as defined by the reference standard does not match the review question? CONCERN: LOW/HIGH/UNCLEAR**

Low risk (1) if the criteria for diagnosis was clearly defined and the target condition diagnosed by a pathologist.

High risk (2) if the criteria for diagnosis was not clearly defined or if the target condition was not diagnosed by a pathologist.

Unclear (3) if the criteria for diagnosis of a given condition was unclear or if it is not clear who diagnosed the target condition.

#### Domain 4: Flow and Timing

##### *Risk of bias (describe the index test and how it was conducted and interpreted)*

###### Signaling questions

1. Was the time interval between diagnosis of the reference standard and the scanning of the glass slides for whole slide images <10 years? Yes/No/Unclear

##### **QUESTION 7 – Could the case flow have introduced bias? RISK: LOW/HIGH/UNCLEAR**

Low risk (1) if answer to signalling question was 'yes'

High risk (2) if answer to signalling question was 'no'

Unclear (3) if answer to signalling question was 'unclear'

## S4 – Individual paper scores for QUADAS-2 assessment

First author	Publication year	Risk of Bias				Concerns of Applicability		
		Patient selection	Index test	Reference standard	Flow and timing	Patient selection	Index test	Reference standard
Aatresh	2021	3	2	3	3	3	1	3
Abdeltawab	2021	1	2	1	3	3	1	1
Achi	2019	2	2	3	3	3	3	3
Alheejawi	2021	3	2	3	1	3	3	3
Ashraf	2022	2	2	1	3	3	1	1
Ba		3	2	1	3	3	1	1
BenTaieb	2017	3	1	1	3	3	1	1
Cengzig	2022	3	3	3	3	3	3	3
Chen	2021	3	1	1	1	3	1	1
Chen	2020	2	1	1	3	3	1	3
Chen	2022	3	2	1	3	3	3	1
Cho	2019	2	3	1	3	3	3	3
Choudhary	2021	2	2	1	3	3	3	3
Coudray	2018	2	2	1	3	3	1	1
Cruz-Roa	2018	3	1	1	3	3	1	3
Cruz-Roa	2017	3	1	1	3	3	1	3
da Silva	2021	1	2	1	1	1	1	1
De Logu	2020	3	2	1	3	3	3	1
Dehkharghanian	2021	2	1	3	3	3	1	1
del Amor	2021	3	2	1	3	3	1	1
DiPalma	2021	3	2	3	3	3	1	2
Duran-Lopez	2021	3	2	3	3	3	3	3
Esteban	2019	2	1	1	3	3	1	3
Feng	2021	2	2	3	3	3	1	2
Fenstermaker	2020	2	2	3	3	3	3	1
Fu	2021	2	1	3	3	3	1	3
Hameed	2020	3	2	3	3	3	1	2
Han	2020a	3	2	1	3	3	1	1
Han	2020b	3	2	1	3	3	1	1
Haryanto	2021	2	2	3	3	3	2	2
Hekler	2019	1	2	1	1	1	1	1
Hohn	2021	3	2	1	3	3	3	1
Huang	2021	1	2	1	2	1	1	1
Iizuka	2020	3	1	1	3	3	1	1
Jin	2020	2	2	3	3	3	1	2
Johny	2021	2	2	3	3	3	1	2
Kanavati	2021	3	1	1	3	3	1	1
Kanavati	2020	3	1	1	3	3	1	1
Khalil	2022	3	2	1	3	3	1	3
Kiani	2020	1	1	1	1	1	1	2
Kimeswenger	2020	3	2	1	3	3	1	1
Li	2021	3	2	1	3	3	1	3
Li	2018	3	2	3	3	3	1	2
Li	2020	3	2	1	1	3	1	1
Lin	2019	2	2	3	3	3	1	2
Litjens	2016	1	2	1	1	1	1	1
Ma	2020	3	2	1	3	3	1	2
Menon	2022	2	2	3	3	3	3	3
Mishra	2017	3	3	1	3	3	3	2
Miyoshi	2020	3	2	1	1	3	2	1
Mohlman	2020	3	2	1	3	3	1	1
Naito	2021	3	2	1	1	3	1	1
Nasir-Moin	2021	2	1	1	1	3	1	1
Noorbakhsh	2020	2	2	3	3	3	1	3
Rasmussen	2020	1	1	1	3	3	1	2
Roy	2021	2	2	3	3	3	3	3
Sabol	2020	2	3	1	3	3	3	2
Sadeghi	2019	2	2	1	3	3	3	2
Sali	2020	3	2	3	1	3	1	3
Schau	2020	3	2	1	3	3	1	1
Schilling	2018	3	2	3	1	3	1	3
Schrammen	2022	3	3	3	3	2	3	3
Shin	2020	2	3	1	3	3	1	2
Song	2013	3	2	3	3	3	3	3
Song	2020	3	1	3	3	3	1	3
Song	2020	1	1	1	1	1	1	1
Steinbuss	2020	3	2	1	3	3	1	1
Steiner	2018	3	1	1	1	3	1	1
Sun	2020	3	2	1	1	3	3	1
Swiderska-Chadaj	2020	3	1	1	3	3	1	2
Syed	2021	3	3	1	2	3	1	1
Syrykh	2020	3	2	1	3	3	1	1
Tabibu	2019	2	2	3	3	3	1	3
Tsuneki	2022	1	1	1	3	3	1	1
Tsuneki	2021	2	2	1	3	2	1	1
Tung	2022	2	2	1	1	3	1	3
Uegami	2022	1	2	1	1	1	1	1
Valkonen	2017	3	2	3	3	3	3	3
Wang KS	2021	3	1	1	3	3	1	3
Wang L	2020	3	1	1	2	3	1	1
Wang Q	2021	2	1	3	3	3	1	3
Wang S	2019	3	2	3	3	3	1	3
Wang X	2020	2	1	3	3	3	1	3
Wang C	2017	2	2	3	3	3	3	3
Wei	2020	3	1	1	1	1	1	1

Wei	2019	3	2	1	1	3	1	1
Wu	2020	3	3	3	3	3	3	3
Xu	2017	2	2	1	3	3	1	3
Xu	2021	2	1	1	3	2	1	3
Yan	2022	2	3	3	3	3	3	3
Yang	2021	3	1	1	3	3	1	1
Yang	2022	3	3	1	3	3	3	2
Yu	2020	2	2	1	3	3	1	1
Yu	2019	2	3	1	3	3	3	1
Yu	2021	3	3	1	3	3	1	1
Zhang	2022	3	3	1	1	2	2	1
Zhao	2021	2	2	3	3	3	1	2
Zheng	2022	3	2	3	3	3	2	2
Zhou	2021	3	1	1	3	3	3	1
Zhu	2021	3	1	1	3	3	1	1

## S5 – Other accuracy / performance metrics for papers not included in the meta-analysis

First author	Publication year	Reported performance (indication of best performance where multiple sets of results)
Abdeltawab	2021	Average accuracy 0.957; sensitivity 0.920; specificity 0.971
Alheejawi	2021	Accuracy 97.7%, precisions 83.22, recall 87.08%, dice 85.10, Jaccard 74.07
Ba	2021	Overall accuracy 0.867. Best chronic atrophic gastritis: AUC 0.91, sens 0.952, spec 0.992, accuracy 0.986. Values given per disease class: Sensitivity 0.790-0.985; Specificity 0.829-1.000.
BenTaleb	2017	Best accuracy Proposed model at 3 levels: 90.0%
Chen	2021	(Best ADC & SCC) ADC AUC 0.9594 (0.9500-0.9689); SCC AUC 0.9414 (0.9243-0.9593)
Chen	2020	(Detecting liver cancer) accuracy 0.960; Precision 0.945; Recall 1.000; F1 score 0.971. 89.6% accuracy for grade prediction
Chen	2022	AUC 0.984 (per slide accuracy tumour detection WIFPS); accuracy 0.903; sensitivity 0.868; specificity 0.946
Coudray	2018	Normal vs tumour AUC 0.993 (0.974-1.0); 3 class at 5x best AUC 0.981 (0.968-0.980)
Cruz-Roa	2018	Dice 0.76 +/- 0.20; PPV 0.72 +/- 0.22; NPV 0.97 +/- 0.05. (TPR 87%, TNR 92%, FPR 8%, FNR 13)
Cruz-Roa	2017	Dice 0.7586 +/- 0.2006; PPV 0.7162 +/- 0.2204; NPV 0.9677 +/- 0.0511
Dehkharghanian	2021	Precision 0.92; Recall 0.91; F1 score 0.91 (average), accuracy 0.86-0.91
del Amor	2021	Sensitivity 0.9285; Specificity 0.9202; PPV 0.8622; NPV 0.9599; F1 score 0.8942; Accuracy 0.9231; AUC 0.9244.
DiPalma	2021	KD (ADv2 model) - Coeliac: Accuracy 87.2, F1 score 75.86, Precision 76.46, Recall 78.0; KD model - Lung: Accuracy 94.18, F1 score 79.63, Precision 79.75, Recall 82.0; KD model - Renal: Accuracy 89.11, F1 Score 77.1, Precision 75.66, Recall 82.64.
Duran-Lopez	2021	Accuracy 94.24%; Sensitivity 98.87%; Precision 90.23%; F1 score 94.33%; AUC 0.94
Feng	2021	Segmentation task: DSC=77.89%, Classification task: AUC=100%
Han	2020	AlexNet-TCM: AUROC=0.964; error rate=6.1%; FNR=15.1%; FPR=5.8%
Haryanto	2021	Best model taken as 300pxx50px overlap. For image classification as malignant: Warwick dataset: sensitivity: 0.69; specificity: 0.93. UI dataset: sensitivity: 0.98; specificity: 1
Huang	2021	Distinguishing cancer from benign epithelium & stroma: AUROC=0.92 (95%CI 0.88-0.95); Cancer detection: weighted k = 0.97 (95%CI 0.96-0.98); Cancer grading: weighted k = 0.98 (95%CI 0.96-1)
Johnny	2021	Accuracy 0.9184; Precision 0.9185; Recall 0.9183; F1 score 0.9183; AUC 0.97 (triangular model)
Khalil	2022	Precision 0.892; Recall 0.837; F1 score 0.844; mIoU 0.749
Kiani	2020	Accuracy 0.885 (0.710-0.960) (CNN alone on internal set); Accuracy 0.842 (0.808-0.876) (CNN alone on external set)
Kimeswenger	2020	Accuracy 0.95; F1 score 0.97; AUC 0.99; Sensitivity 0.96; Specificity 0.93.
Li	2021	AUC 0.971
Lin	2019	FROC (tumour localisation): 0.8533; AUROC (classification): 0.9875.
Ma	2020	AUC 0.9876; accuracy 96%; specificity 93.3%; sensitivity 98.7%
Menon	2022	Accuracy: BRCA=0.97, COAD=0.99, KICH=0.98, KIRP=0.95, LIHC=0.98; LUAD=0.95, LUSC=0.95, PRAD=0.92, READ=0.97, STAD=0.96
Mishra	2017	Accuracy 0.924; Precision 0.97; Recall 0.94; F1-score 0.95
Nasir-Moin	2021	Accuracy model + pathologist best: 80.8% (78.8-82.8)
Noorbakhsh	2020	All tumour types (19) slide level: AUC 0.995 (+/- 0.008). All tumours types tile based: accuracy 0.91 (+/- 0.05); precision 0.97 (+/- 0.02); recall 0.90 (+/- 0.06); specificity 0.86 (+/- 0.07)
Roy	2021	Accuracy 0.922; Precision 0.931; Recall 0.887; F1 score 0.908.
Sabol	2020	CNN Balanced: Accuracy 92.74%; Precision 92.5%; Recall 92.76%; F1 92.64%
Sadeghi	2019	97.8% accuracy on validation set. On testing the 25% quantile of the probability score of the predictions increased from 0.48 to 0.89, and the median of the data increased from 0.95 to 0.99.
Sali	2020	Best model GMM-RF: Average - accuracy 0.952 (0.915-0.989); AUC 0.986 (0.970-1.000); Precision 0.9555 (0.930-0.980); Recall 0.941 (0.903-0.979); F1 score 0.942 (0.904-0.981)
Schilling	2018	Test set: Sensitivity 87.5%; Specificity 80%; PPV 83%; F1 score 88.9%; NPV 100%
Schrammen	2022	AUROC 0.980 (0.975, 0.984) (on training set)
Song	2020	Accuracy 90.4%; AUC 0.92;
Steiner	2018	Sensitivity 91.2% (86-96.5%) P=0.023 (assisted read across images on case basis); AUC 98.5-0.99
Syed	2021	Multi-zoom ResNet50 patch level (same CM): Macro AUC 0.95; Accuracy 95% at patch level, sensitivity 0.96, specificity 0.97, PPV 0.96, NPV 0.97, Precision 0.94, Recall 0.94, F1 score 0.94. Modified ReNet50 with the ensemble: AUC 0.99, Accuracy 98.3%, Sensitivity 95%, Specificity 96%. Multi-zoom ResNet50 biopsy level: AUC 0.99; accuracy 0.98; sensitivity 0.96; Specificity 0.97; PPV 0.96; NPV 0.97; Precision 0.94; Recall 0.94.
Syrykh	2020	AUC 0.99, accuracy 91%
Tabibu	2019	ResNet-18 (KIRC) Cancer v Normal: patch wise accuracy 93.39; Precision 93.41; Recall 92.95; Slide wise AUC 0.99.
Uegami	2022	Test set: Best AUC 0.88 (0.78-0.98). Sensitivity 0.89; Specificity 0.74.
Valkonen	2017	Training: Accuracy 93%; Sensitivity 92.6%; Specificity 93.3%; F-score 0.93. Best AUC 0.98464 (0.97995 - 0.98932) cross validation. Random Forest sensitivity 92.6%, specificity 93.3%, F-score 0.93.
Wei	2020	Int mean: accuracy 93.5%; sensitivity 86.8%; specificity 95.7%. Ext mean: accuracy 87.0%; sensitivity 77.7%; specificity 91.6%
Wei	2019	Kappa score 0.525; average agreement 66.6%; robust agreement 76.7%
Xu	2017	Brain cancer classification (best): Accuracy 97.8%. Segmenting: accuracy 84%. CRC binary best: accuracy 98.0%. CRC multiclass 87.2%.
Yang	2021	EfficientNetB5 on SYSU1 (best): Macro average AUC 0.988 (0.982-0.994); accuracy 0.860; weighted F1 score 0.860
Yang	2022	(FA-MSCN 5x_2.5x) Sensitivity 0.96; Intersection over union (IOU) 0.89
Yu	2020	AUC 0.975 (+/- 0.001) (Tumour detection)
Yu	2019	AUC 0.985 (+/- 0.004) (SCC vs benign); AUC 0.971 (+/- 0.007) (AdenoCa vs benign)
Yu	2021	AUC 0.996 (CI 0.949-0.984) (case level but 1 slide per case)
Zheng	2022	TCGA ext test set normal v tumour: AUC 0.980 (+/- 0.04). 3 label task TCGA: Average accuracy 82.3; average AUC 92.8.
Zhou	2021	Combination framework: Accuracy 0.946, Precision 0.964, Recall 0.982, F1 score 0.973

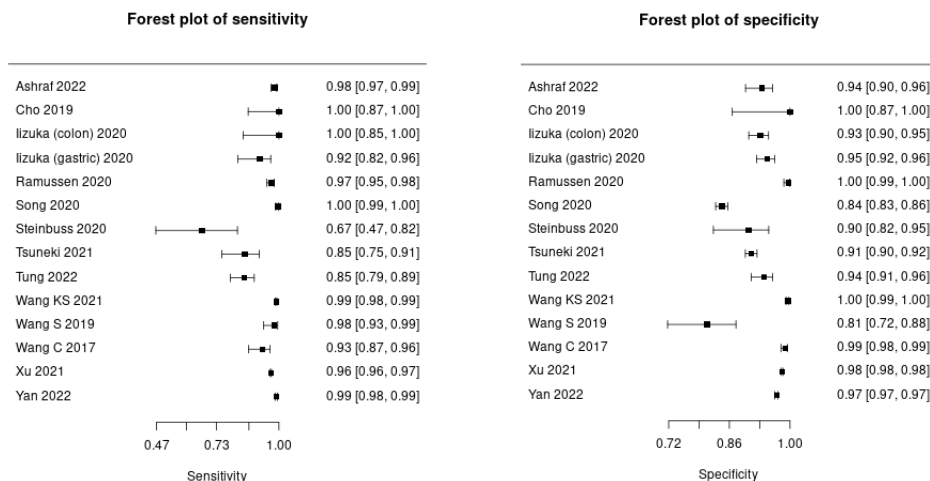
## S6 – Meta analysis: additional data & source of data

Author	TP	FN	FP	TN	N	Sens	Spec
Aatresh 2021	90	3	0	50	143	0.968	1
Achi 2019	176	4	4	56	240	0.978	0.933
Ashraf 2022	485	9	16	231	741	0.982	0.935
Cengzig 2022	63322	9029	5848	23507	101706	0.875	0.801
Cho 2019	25	0	0	25	50	1	1
Choudhary 2021	56333	3311	3289	20325	83258	0.944	0.861
da Silva 2021	173	2	27	377	579	0.989	0.933
De Logu 2020	1074	48	18	773	1913	0.957	0.977
Esteban 2019	16	2	0	1	19	0.889	1
Fenstermaker 2020	12046	0	85	3000	15131	1	0.972
Fu 2021	35	0	0	12	47	1	1
Hameed 2020	86	2	6	76	170	0.977	0.927
Han 2020	32092	5689	70530	1140166	1248477	0.849	0.942
Hekler 2019	38	12	20	30	100	0.76	0.6
Hohn 2021*	60	5	17.4	49.6	132	0.923	0.74
Iizuka (Colon) 2020	21	0	33	446	500	1	0.931
Iizuka (Gastro) 2020	56	5	23	416	500	0.918	0.948
Jin 2020	13435	2949	1999	14385	32768	0.82	0.878
Kanavati 2021	431	127	30	794	1382	0.772	0.964
Kanavati 2020	586	5	41	48	680	0.992	0.539
Li 2018	6944	2	56	998	8000	1	0.947
Li 2020	171	3	24	61	259	0.983	0.718
Litjens (Prostate) 2016	43	2	0	30	75	0.956	1
Litjens (Breast) 2016	16	2	16	40	74	0.889	0.714
Miyoshi 2020	78	1	2	19	100	0.987	0.905
Mohlman 2020	741	101	860	2372	4074	0.88	0.734
Naito 2021	80	6	1	33	120	0.93	0.971
Rasmussen 2020	446	15	2	508	971	0.967	0.996
Schau 2020	16250	4737	4862	5228	31077	0.774	0.518
Shin 2020	594	26	212	408	1240	0.958	0.658
Song 2013	69	13	11	67	160	0.841	0.859
Song 2020	630	3	405	2174	3212	0.995	0.843
Steinbuss 2020	16	8	8	76	108	0.667	0.905
Sun 2020	46	13	0	141	200	0.78	1
Swiderska Chadaj 2020	55	3	4	23	85	0.948	0.852
Tsuneki 2022	695	38	1	33	767	0.948	0.971
Tsuneki 2021	63	11	153	1572	1799	0.851	0.911
Tung 2022	157	28	22	343	550	0.849	0.94
Wang KS 2021	3940	48	9	1842	5839	0.988	0.995
Wang L 2020	60289	5963	1215	15660	83127	0.91	0.928
Wang Q 2021	38	4	3	65	110	0.905	0.956
Wang S 2019	104	2	18	76	200	0.981	0.809
Wang X 2020	170	0	1	14	185	1	0.933
Wang C 2017	116	9	10	865	1000	0.928	0.989
Wu 2020*	17.6	18.4	15.7	376.3	428	0.489	0.96
Xu 2021	19300	700	360	19640	40000	0.965	0.982
Yan 2022	1397	14	267	8322	10000	0.99	0.969
Zhang 2022	1056	26	34	558	1674	0.976	0.943
Zhao 2021	213	13	21	82	329	0.942	0.796
Zhu 2021	904	4	0	9	917	0.996	1

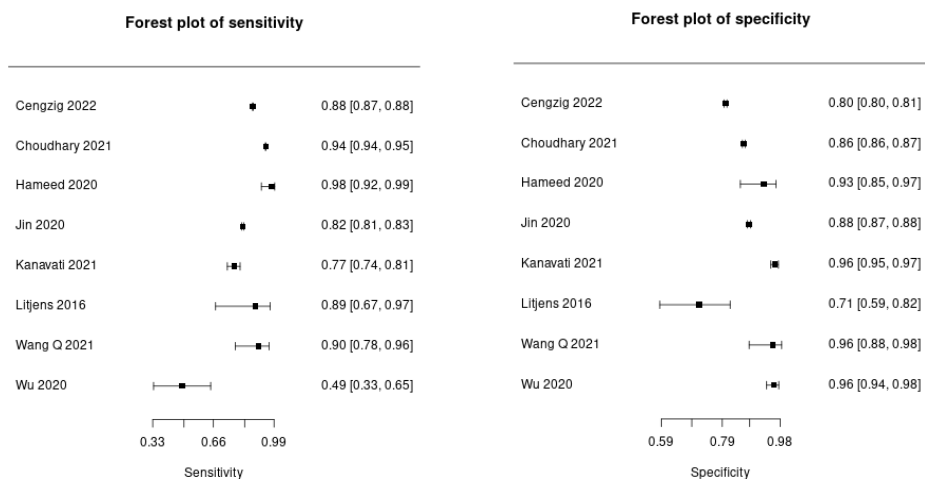
\*Data provided by authors as averages of a cross validation (not whole numbers)

Colour key for source of meta-analysis data	
	Retrieved from study / supplementary materials
	Multiclass confusion matrix in study reduced to 2x2 table
	Back-calculated from data provided in study
	Provided by author
	Back-calculated from data provided by author
	Multiclass confusion matrix provided by author reduced to 2x2 table

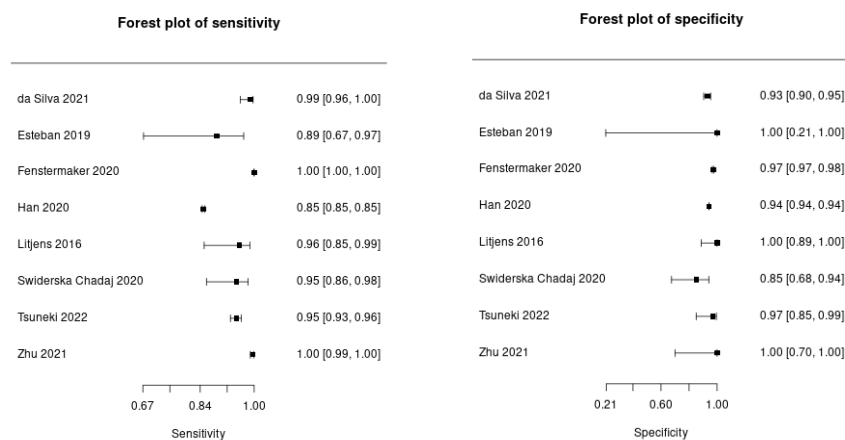
## S7 – Supplementary forest plots of sensitivity and specificity for subgroups



### S7a – Forest plots for sensitivity and specificity in studies of gastrointestinal pathology

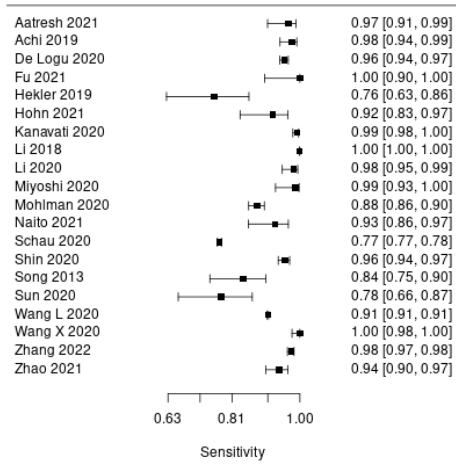


### S7b – Forest plots for sensitivity and specificity in studies of breast pathology

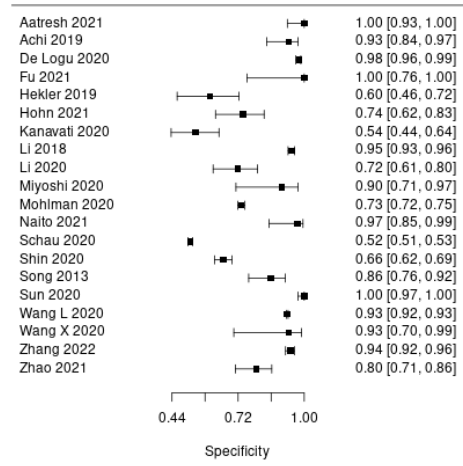


### S7c – Forest plots for sensitivity and specificity in studies of urological pathology

Forest plot of sensitivity



Forest plot of specificity



S7d – Forest plots for sensitivity and specificity in studies of other pathologies

## S8 – Further details of study characteristics

First author	Publication year	Funding source of research	Intended use*	Pathological subspecialty/ies	Total number of slides in study (other units if not provided)	Number of data sources	Is the dataset(s) open source	Is the test set independent of the training set
Aatresh	2021	Science Engineering and Research Board, Department of Science and Technology, Govt. of India	Classifying subtypes of liver cancer (Diagnosis of Sub-types of Liver Cancer)	Hepatobiliary pathology	398 WSI (141 WSI into 705 patches for TCGA), (257 WSI into 1338 patches for KMC)	2	Mixed	Unclear
Abdeltawab	2021	No funder declared	Classifying subtypes of renal cancer (Classify patches into fat, parenchyma, clear cell papillary RCC and clear cell RCC)	Uropathology	64 WSIs	1	No	Yes
Achi	2019	No funder declared	Classifying lymphoma subtypes (Classify images into benign lymph node, diffuse large B cell lymphoma, Burkitt lymphoma, small lymphocytic leukaemia)	Haematopathology	128 WSIs (equalling 2560 40x40 pixel patches)	2	Unclear	Yes
Alheejawi	2021	Natural Sciences and Engineering Research Council of Canada; Ministry of Higher Education and Scientific Research, Iraq; Imam Ja'afar Al Sadiq University, Iraq	Detecting melanoma	Dermatopathology	4 WSIs	1	No	Yes
Ashraf	2022	Seegene Medical Foundation, South Korea	Detecting gastric cancer (Classification of stomach endoscopy specimens and lymph nodes into malignant, benign, dysplasia or uncategorised)	Gastrointestinal pathology	905 WSIs and 327,680 96x96 pixel patches	2	Mixed	Yes
Ba	2021	PLA General Hospital Medical Big Data and Artificial Intelligence Project	Classifying subtypes of gastritis (Gastritis detection and subtyping)	Gastrointestinal pathology	1250 WSIs	1	No	Yes
BenTaieb	2017	Natural Sciences and Engineering Research Council of Canada	Classifying subtypes of ovarian cancer	Gynaecological pathology	133 WSIs	1	Yes	Yes
Cengzig	2022	No funder declared	Detecting breast cancer (Breast cancer classification benign versus malignant)	Breast pathology	398,381 50x50 size patches	Not stated	Unclear	Unclear
Chen	2021	Ministry of Sciences and Technology Taiwan	Classifying subtypes of lung cancer	Cardiothoracic pathology	7003 WSIs hospitals set; 1044 WSIs TCGA test set.	4	Mixed	Yes
Chen	2020	Opening Fund of Engineering Research Center of Cognitive Healthcare of Zhejiang Province, Zhejiang Medical Health Science and Technology Project, National Natural Science Foundation of China	Detecting liver cancer; grading liver cancer severity (Classification of HCC, plus grade, plus mutation status)	Hepatobiliary pathology	592 WSIs	2	Mixed	Yes
Chen	2022	National Key R&D program of China; National Natural Science Foundation of China; Guangdong Natural Science Foundation.	Detecting lung cancer, classifying subtype of lung cancer (Lung cancer histological diagnosis)	Cardiothoracic pathology	1914 cases	3	No	Yes
Cho	2019	National Research Foundation of Korea; Catholic Medical Centre Research Foundation	Detecting gastric cancer (Classification of stomach tissue from non stomach tissue and then classification of stomach tissue patches via 2nd CNN into gastric adenocarcinoma versus normal)	Gastrointestinal pathology	803 WSIs	2	Mixed	Yes
Choudhary	2021	No funder declared	Detecting breast cancer (Classification of breast cancer - invasive ductal carcinoma versus not)	Breast pathology	162 WSIs	1	Yes	Yes
Coudray	2018	Cancer Centre Support Grant, Laura and Isaac Perlmutter Cancer Centre.	Detecting lung cancer & classification of non-small cell lung cancer subtypes (Classification and mutation prediction from NSC lung cancer)	Cardiothoracic pathology	1634 WSIs (TCGA) + 340 WSIs (New York) independent set	2	Mixed	Yes
Cruz-Roa	2018	Administrative Department of Science, Technology and Innovation - Colciencias, Universidad Nacional de Colombia; Universidad de los Llanos; the National Cancer Institute of the National Institutes of Health; National Institute of Diabetes and Digestive and Kidney Diseases; National Center for Research Resources; United States Department of Defense Prostate Cancer Synergistic Idea Development Award; United States	Detecting breast cancer (Detecting presence and extent of invasive breast cancer)	Breast pathology	945 cases	4	Mixed	Yes

		Department of Defense Lung Cancer Idea Development New Investigator Award; United States Department of Defense Prostate Cancer Idea Development Award; United States Department of Defense Peer Reviewed Cancer Research Program Case Comprehensive Cancer Center Pilot Grant; VelaSano Grant, Cleveland Clinic; the Wallace H. Coulter Foundation Program Case Western Reserve University.						
Cruz-Roa	2017	DGI-Unillanos; Administrative Department of Science, Technology and Innovation of Colombia; National Cancer Institutes of the National Institutes of Health; the National Institute of Diabetes and Digestive and Kidney diseases; National Center for Research Resources; DOD Prostate Cancer Synergistic Idea Development Award; DOD Lung Cancer Idea Development New Investigator Award; DOD Prostate Cancer Idea Development Award; DOD Peer Reviewed Cancer Research Program; Cleveland Clinic; Wallace H. Coulter Foundation Program, Case Western Reserve University.	Detecting breast cancer (Detecting presence and extent of invasive breast cancer)	Breast pathology	605 patients	4	Mixed	Yes
da Silva	2021	Paige; Breast Cancer Research Foundation; National Institutes of Health / National Cancer Institute; P50 grant;	Detecting prostate cancer (Classification of prostate biopsies into benign and suspicious specimens )	Uropathology	661 WSIs (from 579 unique needle core biopsy parts	1	No	Yes
De Logu	2020	Associazione Italiana per la Ricerca sul Cancro	Detecting melanoma (Segment H&E WSIs into melanoma & healthy tissue)	Dermatopathology	100 WSIs	3	No	Yes
Dehkharghanian	2021	Government of Ontario, Canada and the Ontario Research Fund-Research Excellence Gigapixel image identification consortium	Classifying lung cancer subtypes	Cardiothoracic pathology	758 WSIs	2	Mixed	Yes
del Amor	2021	Horizon 2020, the Spanish Ministry of Economy and Competitiveness, Instituto de Salud Carlos III, GVA, Polytechnic University of Valencia, Marie Skłodowska Curie grant	Detecting spitzoid melanocytic lesions (ROI selection and malignancy prediction in spitzoid melanocytic lesions)	Dermatopathology	53 WSIs	1	No	Yes
DiPalma	2021	US National Library of Medicine, US National Cancer Institute	Detecting coeliac disease; classifying lung cancer subtypes; classifying renal cancer subtypes (Classification of coeliac disease versus non-specific duodenitis and coeliac sprue, classification of lung adenocarcinoma into 5 classes (lepidic, acinar, papillary, micropapillary and solid) and classification of RCC into 3 subtypes (chromophobe, papillary and clear cell))	Multiple	Coeliac: 1364 patients; Lung: 269 WSIs; Renal 882 WSIs.	2	Mixed	Yes
Duran-Lopez	2021	Spanish Agencia Estatal de Investigación, European Regional Development Fund	Detecting prostate cancer (Classification of prostate cancer versus normal)	Uropathology	332 WSIs	1	No	Unclear
Esteban	2019	Ministerio de Economía y Competitividad.	Detecting prostate cancer (Classification of prostate cancer)	Uropathology	79 WSIs from SICAPv1; and ext set 593 patches for testing from Gertych et al	1	Mixed	Yes
Feng	2021	National Key Research and Development Program of China; National Natural Science Foundation of China; Zhejiang University Education Foundation; Zhejiang public welfare technology research project; Key Laboratory of Medical Neurobiology of Zhejiang Province; NSF Grant.	Detecting colorectal cancer (Segmentation and classification of colorectal cancer (malignant vs benign))	Gastrointestinal pathology	1000 WSIs	1	Yes	Yes
Fenstermaker	2020	No funders declared	Detecting renal cell cancer. Classifying subtypes of RCC. (Also grading of RCC)	Uropathology	42 patients	1	Yes	Yes
Fu	2021	Foundation of Beijing Municipal Science and Technology Commission; National Key Research and Development Program of China; National Natural Science Foundation of China.	Detecting pancreatic ductal adenocarcinoma (detection and classification of pancreatic ductal adenocarcinoma (PDAC) (cancer vs non-cancer))	Hepatobiliary pathology	283 WSIs	2	Mixed	Yes
Hameed	2020	Basque Country project MIFLUDAN; eVida Research Group IT 905-16 (University of Deusto, Spain)	Detecting breast cancer (classification of breast cancer (carcinoma vs non-carcinoma))	Breast pathology	845 areas/patches from 544 WSIs.	1	No	Yes
Han	2020	No funders declared	Detecting prostate cancer. (Also grading prostate cancer)	Uropathology	299 WSIs	1	No	Yes

Han	2020	Canadian Institute of Health Research; Ontario Institute for Cancer Research; Prostate Canada; Natural Sciences and Engineering Research Council of Canada	Detecting prostate cancer (Classification of prostate cancer)	Uropathology	299 WSIs	1	No	Yes
Haryanto	2021	Ministry of Research and Technology, Republic of Indonesia	Detecting colorectal cancer (classification of colorectal cancer (malignant vs benign))	Gastrointestinal pathology	165 images + other images from University of Indonesia. (For best model (300px + 50px overlap), no. of CSW-generated images = 13,576 (2,984 (Warwick), 10,592 (UI))	2	Mixed	Unclear
Hekler	2019	No funders	Detecting melanoma (Classification task melanoma versus nevi)	Dermatopathology	695 WSIs from 595 patients	1	No	Yes
Hohn	2021	Federal Ministry of Health, Berlin, Germany; Tumour Behaviour Prediction Initiative.	Detecting melanoma (Classify H&E WSIs into melanoma & benign naevus)	Dermatopathology	431 WSIs	2	No	Yes
Huang	2021	PathomIQ	Detecting prostate cancer. (Also grading prostate cancer and volume quantification)	Uropathology	1000 WSIs	1	No	Yes
Iizuka	2020	No funders declared	Classifying gastric and colonic tumours (classification of epithelial tumours of stomach & colon into adenocarcinoma, adenoma, and non-neoplastic.)	Gastrointestinal pathology	10,186 WSIs	2	Mixed	Yes
Jin	2020	CancerCare Manitoba Foundation; Natural Sciences and Engineering Research Council of Canada; University of Manitoba; Manitoba Medical Services Foundation Allen Rouse Basic Science Career Development Research Award.	Detecting breast cancer metastases in lymph nodes	Breast pathology	327,680 patches (PCaM), 438 images (second dataset), 100 patches from 10 WSIs (Warwick)	3	Yes	Yes
Johny	2021	No funders declared	Detecting breast cancer metastases in lymph nodes (detection and classification of breast cancer metastases in lymph nodes (benign vs malignant))	Breast pathology	327,680 patches from 400 WSIs	1	Yes	Yes
Kanavati	2021	No funders declared	Detecting breast cancer and DCIS (classification of breast cancer (ductal carcinoma in situ (DCIS), invasive ductal carcinoma (IDC), benign))	Breast pathology	3672 WSIs	2	No	Yes
Kanavati	2020	Research Institute for Information Technology, Kyushu University	Detecting lung cancer (classification of lung cancer (lung carcinoma vs non-neoplastic))	Cardiothoracic pathology	5734 WSIs	4	Mixed	Yes
Khalil	2022	Ministry of Science and Technology of Taiwan	Detecting breast cancer metastases in lymph nodes (detection/segmentation of breast cancer metastases in lymph nodes)	Breast pathology	188 WSIs (94 H&E, 94 matching IHC CK(AE1/AE3) WSIs)	1	No	Yes
Kiani	2020	Department of Pathology (Stanford University) Stanford Machine Learning Group and the Stanford Center for Artificial Intelligence in Medicine & Imaging	Classification of liver tumour subtypes (classification of liver cancer (hepatocellular carcinoma vs cholangiocarcinoma))	Hepatobiliary pathology	150 WSIs	2	Mixed	Yes
Kimeswenger	2020	ERC; REA; Promedica Stiftung; Swiss Cancer Research Foundation; Clinical Research Priority Program (CRPP), University of Zurich; Swiss National Science Foundation; European Academic of Dermatology and Venereology.	Detecting basal cell carcinoma	Dermatopathology	820 WSIs	2	No	Yes
Li	2021	The National Key Research and Development Program of China; Natural Science Foundation of China; Hunan Province Science Foundation; Changsha Municipal Natural Science Foundation; Scientific Research Fund of Hunan Provincial Education Department.	Detecting melanoma (Lesion detection & distinguish between melanoma, intradermal naevi, junctional naevi, compound naevi & normal tissue)	Dermatopathology	701 WSIs	2	Mixed	Yes
Li	2018	No funder declared	Classifying subtypes of brain tumour	Neuropathology	206 WSIs	1	No	Yes
Li	2020	No funder declared	Detecting thyroid cancer (classification of thyroid nodules (benign, uncertain, malignant))	Head & neck pathology	608 WSIs	1	No	Yes

Lin	2019	Hong Kong Innovation and Technology Commission; Hong Kong Research Grants Council; Global Partnership Fund, University of Warwick.	Detect breast cancer metastases in lymph nodes (detection and classification of breast cancer metastases in sentinel lymph nodes)	Breast pathology	400 WSIs	1	Yes	Yes
Litjens	2016	SiTPro Foundation	Detecting breast cancer metastases in sentinel lymph nodes & prostate cancer grading	Multiple	Prostate: 225 WSIs; Breast: 271 WSIs.	1	No	Yes
Ma	2020	Shanghai Science and Technology Committee; National Key R&D Program of China; National Natural Science Foundation of China; Cross-Institute Research Fund of Shanghai Jiao Tong University; Innovation Foundation of Translational Medicine of Shanghai Jiao Tong University School of Medicine; Technology Transfer Project of Science & Technology, Department of Shanghai Jiao Tong University School of Medicine	Detecting gastric cancer and classifying gastric disease (detection and classification of mucosal lesions of the stomach (normal mucosa, chronic gastritis, and intestinal-type gastric cancer (GC))	Gastrointestinal pathology	763 WSIs	1	No	Yes
Menon	2022	Ihub-Data, International Institute of Information and Technology, Hyderabad	Detect multiple cancer types (classification of cancer vs normal for 11 cancer subtypes across 7 organs (breast, colorectal, kidney, liver, lung, prostate, stomach))	Multiple	9792 WSIs	1	Yes	Yes
Mishra	2017	Cancer Prevention and Research Institute of Texas (CPRIT)	Detecting osteosarcoma (classification of osteosarcoma in image tiles (tumour, necrosis, nontumour))	Soft tissue & bone pathology	82 WSIs (64,000 patches)	Unclear	No	Yes
Miyoshi	2020	Chugai Pharmaceutical Co. Ltd	Classify subtypes of Lymphoma (diffuse large B-cell lymphoma (DLBCL), follicular lymphoma (FL), and reactive lymphoid hyperplasia (RLH))	Haematopathology	388 sections	1	No	Yes
Mohlman	2020	No funder declared	Classify subtypes of lymphoma (Burkitt lymphoma (BL) vs diffuse large B-cell lymphoma (DLBCL))	Haematopathology	10,818 patches from unknown no. slides (70 cases)	2	No	Yes
Naito	2021	Research Institute for Information Technology Kyushu University	Detecting pancreatic ductal adenocarcinoma	Hepatobiliary pathology	532 WSIs	1	No	Yes
Nasir-Moin	2021	National Cancer Institute; National Library of Medicine	Assisting the pathologist with classifying subtypes of colorectal polyp	Gastrointestinal pathology	846 WSIs used in experiment + 60 WSIs for other purposes	25	No	Yes
Noorbakhsh	2020	NIH Cloud Credits Model Pilot, NIH Big Data to Knowledge (BD2K) program; Google Cloud; NCI grant.	Detecting multiple cancer types and subtype classification (Classification of tumour/non tumour)	Multiple	29,930 WSIs	2	Yes	Yes
Rasmussen	2020	Nova Scotia Health Authority Research Fund	Detecting hereditary diffuse gastric cancer (Computer-assisted diagnosis of hereditary diffuse gastric cancer)	Gastrointestinal pathology	17,636 patches	2	No	Yes
Roy	2021	No funders	Detecting invasive ductal carcinoma of the breast	Breast pathology	162 WSIs; 277,524 patches	1	Yes	Unclear
Sabol	2020	A4EU project from European Union's Horizon 2020 research & innovation programme; Maria Currie RISE LIFEBOOTS Exchange Grant; EU FlagEra Joint Project Robocom++, 2017-2021	Detecting colorectal cancer (Explainable classification of colorectal cancer)	Gastrointestinal pathology	5000 tiles	1	Yes	Unclear
Sadeghi	2019	BMBF grant	Detecting lymph node breast cancer metastases	Breast pathology	500 WSI (cameylon 17) + 20,000 patches (cameylon 16)	2	Yes	Yes
Sali	2020	National Institute of Diabetes and Digestive and Kidney Diseases of the National Institutes of Health.	Detecting dysplastic barretts oesophagus and non-dysplastic barretts oesophagus (Identifying dysplastic and non-dysplastic Barretts's Oesophagus)	Gastrointestinal pathology	650 WSI	1	Unclear	Yes
Schau	2020	National Cancer Institute; OHSU Center for Spatial Systems Biomedicine; Knight Diagnostic Laboratories; Biomedical Innovation Program Award, Oregon Clinical and Translational Research Institute.	Detecting liver metastasis and classifying origin site of liver metastases (Predicting primary site of secondary liver cancer)	Gastrointestinal pathology	285 WSIs	1	Unclear	Yes
Schilling	2018	No funder declared	Detecting Hirsprungs disease (Diagnosing aganglionic megacolon (Hirschsprungs disease))	Paediatric pathology	307 WSIs	1	Yes	Yes
Schrammen	2022	German Federal Ministry of Health; Max-Eder-Programme of the German Cancer Aid; NIHR; Yorkshire Cancer Research	Detecting colorectal cancer (Cancer	Gastrointestinal pathology	3337 cases	2	No	Yes

		program; German Research Foundation; Interdisciplinary Research Program of the National Centre for Tumour Diseases, Germany; German Federal Ministry of Education and Research.	detection and prediction of genotype)					
Shin	2020	Ministry of Trade, Industry & Energy (Korea); Ministry of Health & Welfare (Korea)	Detecting ovarian cancer	Gynaecological pathology	10,296 patches, 174 patients + 58 cases for additional experiments	2	Mixed	Yes
Song	2013	Basic Science Research Program, National Research Foundation of Korea, funded by the Ministry of Education, Science and Technology; INHA University Research Grant	Classifying types of pancreatic neoplasm (Automated differentiation between pancreatic serous and mucinous cystadenomas, using proposed set of features)	Hepatobiliary pathology	11 WSIs, 400 patches	1	No	Unclear
Song	2020	CAMS Innovation Fund for Medical Sciences; National Natural Science Foundation of China (NSFC); Tsinghua Initiative Research Programme.	Detecting colorectal adenomas	Gastrointestinal pathology	579 WSIs	3	No	Yes
Song	2020	National Natural Science Foundation of China; CAMS Innovation Fund for Medical Sciences; Medical Big Data and Artificial Intelligence Project of the Chinese PLA General Hospital; Tsinghua Initiative Research Program Grant; Beijing Hope Run Special Fund of Cancer Foundation of China.	Detecting gastric cancer (Pixel level cancer detection - to support pathologist in diagnostic review)	Gastrointestinal pathology	8153 WSIs	2	No	Yes
Steinbuss	2020	No Funders	Classify subtypes of gastritis (Classification of the most common gastritis subtypes A, B and C.)	Gastrointestinal pathology	1230 patches	1	No	Yes
Steiner	2018	Google Brain Healthcare Technology Fellowship	Assist pathologist in detecting breast cancer metastases in lymph nodes	Breast pathology	339 WSIs	3	Mixed	Yes
Sun	2020	National Basic Research Program of China; Science and Technology Major Project of Hubei Province (Next-Generation AI Technologies); Medical Science and Technology projects of China	Detecting endometrial cancer; classifying endometrial diseases	Gynaecological pathology	3502 patches	1	Mixed	Yes
Swiderska-Chadaj	2020	Philips Digital and Computational Pathology	Detecting prostate cancer (Whole slide classification of prostate cancer)	Uro pathology	717 WSIs	3	No	Yes
Syed	2021	National Institute of Diabetes and Digestive and Kidney Diseases of the National Institutes of Health, Bill and Melinda Gates Foundation, University of Virginia Center for Engineering in Medicine, University of Virginia THRIV Scholar Career Development Award.	Detecting coeliac disease and environmental enteropathy	Gastrointestinal pathology	461 WSIs	3	No	Yes
Syrykh	2020	No funder declared	Detecting follicular lymphoma (Automate differential diagnosis between follicular lymphoma and follicular hyperplasia)	Haematopathology	491 WSIs (378 + 65 + 24 +24)	2	No	Yes
Tabibu	2019	No funder declared	Detecting renal cancer and classifying subtype	Uro pathology	2105 WSIs	1	Yes	Yes
Tsuneki	2022	No funders	Detect prostate cancer (Prostate carcinoma classification in needle biopsies)	Uro pathology	3694 WSIs	6	Mixed	Yes
Tsuneki	2021	No funders	Detecting poorly differentiated colorectal cancer (Classification of diffuse type/poorly differentiated ADC in endoscopic biopsy specimen whole slide images)	Gastrointestinal pathology	2547 WSIs	5	No	Yes
Tung	2022	No funders declared	Detecting gastric cancer	Gastrointestinal pathology	50 patients; 2750 image tiles.	1	Yes	Yes
Uegami)	2022	New Energy and Industrial Technology Development Organization (NEDO)	Detecting Usual Interstitial Pneumonia (UIP) (Diagnosing interstitial lung disease (interstitial pneumonia))	Cardiothoracic pathology	715 WSIs + 181 WSIs pretraining set	1	No	Yes
Valkonen	2017	1. Academy of Finland 2. Tekes - The Finnish Funding Agency for Innovation 3. Cancer Society of Finland, Sigrid Juselius Foundation and Doctoral Programme of Computing and Electrical Engineering, Tampere University of Technology	Detecting breast cancer metastases in lymph nodes	Breast pathology	270 WSIs	1	Yes	Unclear
Wang KS	2021	1. National Institutes of Health 2. Edward G. Schlieder Endowment and the Drs. W. C. Tsai and P. T. Kung Professorship in Biostatistics from Tulane University 3. National Key Research and Development Plan of China 4. National Natural Science	Detecting colorectal cancer (Diagnosis of CRC)	Gastrointestinal pathology	14,680 WSIs	14	Mixed	Yes

		Foundation of China 5. Jiangwang Educational Endowment. 6. Natural Science Foundation of Hunan Province						
Wang L	2020	National Natural Science Foundation of China	Detect eyelid melanoma (Detect melanoma in H&E WSIs of eyelid specimens)	Dermatopathology	155 WSIs (83,126 patches)	2	No	Yes
Wang Q	2021	National Natural Science Foundation of China, National Key R&D Program of China, Key R&D Program of Liaoning Province, Young and Middle-aged Talents Program of the National Civil Affairs Commission, Liaoning BaiQianWan Talents Program, University-Industry Collaborative Education Program.	Detecting breast cancer metastases in lymph nodes (Classification of WSI)	Breast pathology	529 WSIs	2	Yes	Yes
Wang S	2019	Hong Kong Innovation and Technology Commission; Shenzhen Science and Technology Program.	Classification of gastric cancer and dysplasia	Gastrointestinal pathology	608 WSIs	1	No	Yes
Wang X	2020	Hong Kong Innovation and Technology Commission; National Natural Science Foundation of China; Shenzhen Science and Technology Program.	Classifying subtypes of lung cancer	Cardiothoracic pathology	1439 WSIs (939 WSI internal, 500 WSI external)	2	Mixed	Yes
Wang C	2017	National Natural Science Foundation of China	Detecting colorectal cancer (Classification of 8 tissue types (tumour, simple stroma, complex stroma, immune, debris, mucosal, adipose, background))	Gastrointestinal pathology	10 WSIs (1000 150 x 150 pixel images)	1	Yes	Unclear
Wei	2020	NIH; Geisel School of Medicine at Dartmouth; Norris Cotton Cancer Centre.	Classification of colorectal polyps	Gastrointestinal pathology	746 WSIs	2	No	Yes
Wei	2019	No funders declared	Classification of lung adenocarcinoma histological patterns (Classification of lung cancer subtypes)	Cardiothoracic pathology	422 WSIs	1	No	Yes
Wu	2020	Information Technology for Cancer Research program and National Institutes of Health	Detecting breast cancer (Diagnose ROI in WSI biopsy breast cancer)	Breast pathology	240 cases	1	No	Unclear
Xu	2017	Microsoft Research; Beijing National Science Foundation in China; Technology and Innovation Commission of Shenzhen in China; Beijing Young Talent Project in China; Fundamental Research Funds for the Central Universities of China from the State Key Laboratory of Software Development Environment in Beihang University in China.	Detecting & classifying brain cancer. Detecting colorectal cancer (Classification and segmentation of histopathology images)	Multiple	brain 141 images, colon 717 cropped regions	2	Mixed	Yes
Xu	2021	Guangzhou Key Medical Discipline Construction Project Fund; Guangzhou Science and Technology Plan Project; Guangdong Provincial Science and Technology Plan Project.	Detecting colorectal cancer (Classification of CRC)	Gastrointestinal pathology	476 WSIs (263 + 218 -5 removed)	2	Mixed	Unclear
Yan	2022	Science and Technology Innovation 2030-Key Project of China; Key-Area Research and Development Program of Guangdong Province, China.	Detecting colorectal cancer and colorectal polyps, detecting breast cancer lymph node metastases.	Multiple	NCT-CRC 100,000 patches. CAMELYON1 6 100,000 patches. In-house 20 patients.	3	Mixed	Unclear
Yang	2021	National Key R&D Program of China; National Natural Science Foundation of China; Guangdong Natural Science Foundation; Support Scheme of Guangzhou for Leading Talents in Innovation and Entrepreneurship.	Classifying subtypes of lung cancer and other lung diseases (histopathological WSI classification for lung cancer and mimics)	Cardiothoracic pathology	1693 WSIs	3	Mixed	Yes
Yang	2022	Ministry of Science and Technology (MOST), Taiwan	Detecting hepatocellular carcinoma (Automatic liver tumor detection)	Hepatobiliary pathology	46 WSIs	Unclear	Unclear	Yes
Yu	2020	Schlager Family Award for Digital Health Innovations; Partners' Innovation Discovery Grant; Blavatnik Centre for Computational Biomedicine Award; Harvard Data Science Fellowship.	Detecting serous ovarian carcinoma & predicting tumour grade (Identify grade, subtype and response to platinum-based chemotherapy in serous ovarian carcinoma)	Gynaecological pathology	1375 WSIs	1	Yes	Yes
Yu	2019	National Cancer Institute; National Institutes of Health; National Human Genome Research Institute; National Institutes of Health; Mobilize Centre, Stanford University; Harvard Data Science Fellowship; Harvard Medical School Centre for Computational Biomedicine Award	Detecting lung cancer and classifying subtypes of lung cancer (Identify the types and gene expression subtypes of NSCLC)	Haematopathology		2	Yes	Yes
Yu	2021	No funders	Detecting T cell lymphomas & classifying T cell lymphoma subtypes	Haematopathology	40 WSIs (1 per patient, 33 ROIs)	17	No	Yes
Zhang	2022	Children's Cancer Fund of Dallas, the QuadW Foundation, the NIH grants NCI National Clinical Trials Network (NCTN) Operations Centre, NCTN SDC, Children's Oncology Group (COG) Biospecimen Bank,	Classifying subtypes of rhabdomyosarcoma (Classification) and survival outcome	Soft tissue & bone pathology	272 WSIs	1	Unclear	Yes

		the Cancer Prevention and Research Institute of Texas.	prediction of rhabdomyosarcoma					
Zhao	2021	Major Research Plan of the National Natural Science Foundation of China, the Shanghai Hospital Development Centre Clinical Science and Technology Innovation project, the National Key R&D Program of China and the National Natural Science Foundation of China.	Detecting lung cancer and classifying subtypes of lung cancer (NSCLC subtype classification)	Cardiothoracic pathology	2125 WSIs	1	Yes	Yes
Zheng	2022	National Institutes of Health, Johnson & Johnson Enterprise Innovation Inc., American Heart Association, Karen Toffler Charitable Trust, National Science Foundation.	Detecting lung cancer and classifying lung cancer subtypes (Distinguish lung adenocarcinoma (LUAD) and squamous cell carcinoma (LSCC) from adjacent non-cancerous tissue (normal))	Cardiothoracic pathology	4153 WSIs for train / validate / test + 665 WSIs used for earlier development	3	Yes	Yes
Zhou	2021	Double-Class University project, the National Natural Science Foundation of China, and Postgraduate Research & Practice Innovation Program of Jiangsu Province	Detecting colorectal cancer (classification and localization of colorectal cancer WSI)	Gastrointestinal pathology	1396 WSIs	4	Mixed	Yes
Zhu	2021	US National Library of Medicine; US National Cancer Institute	Classify renal tumour subtypes	Uropathology	1482 WSIs	2	Mixed	Yes

\*Given the varied language used to describe intended use, these were broadly categorised into detecting disease or classifying subtypes of disease for those relevant to this study.